METRICA
METRology Institutional CAtalog

ISTITUTO NAZIONALE DI RICERCA METROLOGICA
Repository Istituzionale

Material sources of the Roman brick-making industry in the I and II century A.D. from Regio IX, Regio XI and Alpes Cottiae

This is the author's accepted version of the contribution published as:

Original
Material sources of the Roman brick-making industry in the I and II century A.D. from Regio IX, Regio XI and Alpes Cottiae / R., Scalenghe; F., Barello; F., Saiano; Ferrara, Enzo; C., Fontaine; L., Caner; Olivetti, ELENA SONIA; I., Boni; S., Petit. - In: QUATERNARY INTERNATIONAL. - ISSN 1040-6182. - 357:(2015), pp. 189-206. [http://dx.doi.org/10.1016/j.quaint.2014.11.026]

Availability:
This version is available at: 11696/34721 since: 2021-03-10T19:01:01Z

Publisher:
Elsevier

Published
DOI:http://dx.doi.org/10.1016/j.quaint.2014.11.026

Terms of use:

This article is made available under terms and conditions as specified in the corresponding bibliographic description in the repository

Publisher copyright

(Article begins on next page)

12 October 2024

Material sources of the Roman brick-making industry in the I and II century A.D. from *Regio IX*, *Regio XI* and *Alpes Cottiae*

R. Scalenghe[ad], F. Barello[b], F. Saiano[a], E. Ferrara[c], C. Fontaine[d], L. Caner[d], E. Olivetti[c], I. Boni[e], S. Petit[d]

[a] Università degli Studi di Palermo, SAF, Palermo, Italy
[b] Soprintendenza per i Beni Archeologici del Piemonte e del Museo Antichità Egizie, Torino, Italy
[c] Istituto Nazionale di Ricerca Metrologica, Torino, Italy
[d] Université de Poitiers, UMR 7285 IC2MP HydrASA, Poitiers, France
[e] Istituto per le Piante da Legno e l'Ambiente, Torino, Italy

Abstract

Bricks, fine pottery, ceramic gears and tiles are among the human-made objects routinely recovered in archaeological documentation. Sites associated with early civilizations can provide thousands of samples from a single excavation. They come in endless varieties according to economic and social circumstances and, as debris can last almost forever, provide important clues about the past behaviours in human societies. Any information about the provenance of ceramics is highly valuable in archaeological analysis. In the case of Roman brick-making, the provenance and manufacture of clayey materials are usually interpreted only by studying stamps imprinted on the artefacts, when available. In this paper, the making of bricks, tiles and other ceramics for building purposes is investigated, in relation to the possible sources of raw materials used for the industry. The major questions to be solved relate to the sites from where the Romans collected the raw materials, the technologies they applied to make bricks and other clayey building materials, and how far have they transported raw resources and final products – *i.e.* mainly bricks and tiles – after furnace treatments, considering that a crucial point was the nearby availability of timber, water, and sandy soils without stones. Some achievements to classify artefacts with identical provenance have been obtained, using the structural transformations induced in the material by thermal treatments of pottery. Comparisons have been made of the trace elements chemical composition in ICP-MS and some physical properties, including magnetic, VSM hysteresis loops, and mineralogical features with XRD and IR analysis, have been identified as proxies to elucidate the possible provenance of rough materials, and appreciate the technologies used by the Roman brick-making industry.

Keywords

Sesquipedalian brick, M•A•[H] stamp, Soil, Rare earth elements, Magnetism, Industria

1. Introduction

Brick represents artefacts routinely recovered in the archaeological documentation (Skibo and Feinman, 1999, Hodder, 2012). Their main constituents are fired soils. The exploitation of bricks and tiles has always been very convenient and useful for humankind, as the raw material is abundant on the earth's surface and easy to shape and fire. Yet, little is known of the making of less refined ceramics, whose enormity of production and trade is surprising in view of the slight knowledge we have of the associated industry. This is the case for bricks and tiles in the Roman age, whose production was one of the most vital manufacturing industries in Roman times with confirmed evidence of export towards the main cities of the Mediterranean (Helen, 1975, Thébert, 2000). Nevertheless, the technological aspects of brick making in ancient Rome, which is thought to have been one of the most important businesses of the Empire, remain relatively mysterious. Some major questions are related to defining from where the Romans collected the raw

materials, how have they made their bricks, and how far have they transported the bricks with respect to the furnaces.

In general, the determination of provenance of archaeological finds is based on two assumptions: i) raw materials from diverse sources have different chemical compositions; ii) variations of composition within one source are smaller than between materials from different sources. In the archaeological context, the scientific literature illustrates a wide variety of approaches applied in the study and characterization of soils (Facchinelli et al., 2001, Marra et al., 2011) and ceramics artefacts to gain information on provenance, technology and manufacture, from X-ray diffraction (*e.g.* Rye, 1981), and direct observation of structural phases by scanning electron microscopy, and reflection spectroscopic investigation of the colour of ceramics (Marra et al., 2011, López-Arce et al., 2003, Calliari et al., 2001, Hatcher et al., 1994, Marengo et al., 2005).

To investigate the manufacture of bricks and tiles in the Roman territory during the first centuries AD and investigate how the sources of raw materials were selected, we analysed the soil features of an area situated by the Po river in northwestern Italy – in particular, the triangle between two ancient Roman regions (*Liguria*, *Transpadana*) and one Alpine district (*Alpes Cottiae*) – along with the different chemical and physical properties of soils, bricks, and tiles recovered from Roman sites located in the same region. Chemical, structural and magnetic analysis were conducted, respectively, using mass spectrometry coupled with inductively coupled plasma (ICP-MS), X-ray diffraction (XRD), infrared spectroscopy (IR), and magnetic measurements.

2. Material and methods

2.1. Spatial and temporal domain – sampling

Since the Julio-Claudian epoch (0–35 BC) and for census requirements, the Italian territory was divided by Roman government into *Regiones*. Northwestern Italy corresponded to *Regio IX Liguria*, *Regio XI Transpadana*, and *Alpes Cottiae*, with borders (Fig. 1) defined by *Alpes Maritimae* (southwest), *Gallia Narbonensis* (west).

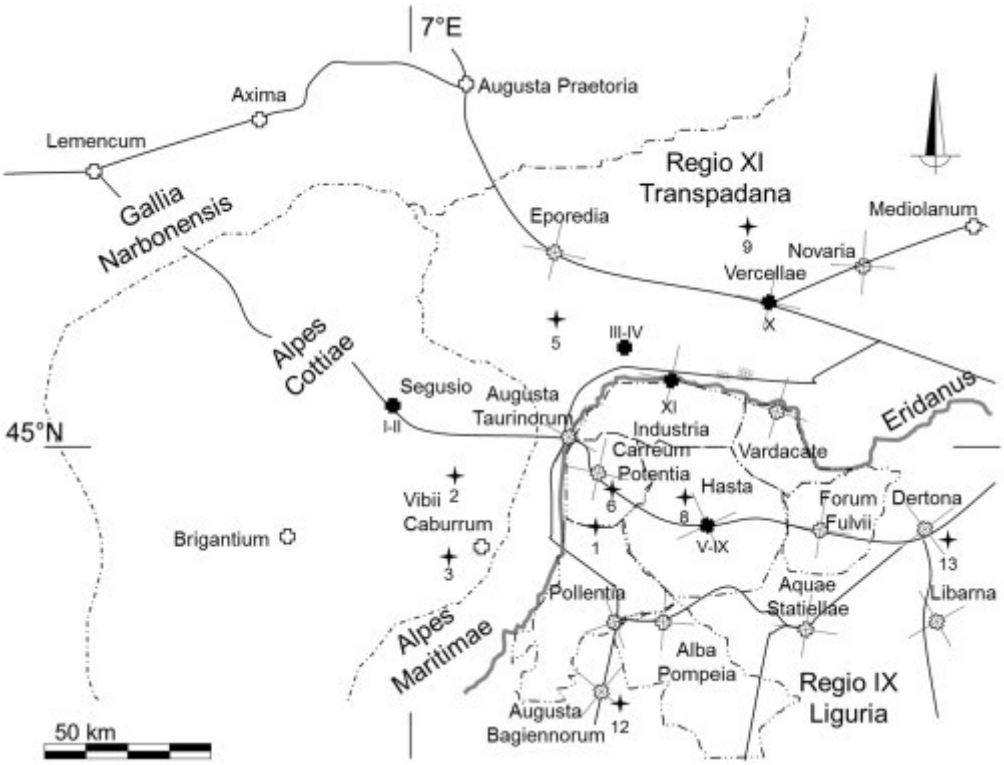

Fig. 1. Northwestern Italian territories controlled by Romans during Augustus' times and locations of sites described in this paper (archaeological samples, filled crosses and soil samples, filled stars). *Regio IX* and *XI* were separated by the river *Eridanus*, Po in

grey. The province of Cottian Alps secured the communications over the Alpine passes, its capital was Segusio (Susa). The cities of *Lemencum*, Chambéry, *Augusta Praetoria*, Aosta, *Eporedia*, Ivrea, *Vercellae*, Vercelli, *Novaria*, Novara, *Mediolanum*, Milan, *Augusta Taurinorum*, Turin, *Brigantium*, Briançon, *Forum Vibii Caburrum*, Cavour, *Carreum Potentia*, Chieri, Vardacate, Casale Monferrato, *Hasta*, Asti, *Pollentia*, Pollenzo, *Forum Fulvii*, near to Alessandria, *Dertona*, Tortona, *Aquae Statiellae*, Acqui Terme, *Alba Pompeia*, Alba, *Augusta Bagiennorum*, close to Bene Vagienna exist today. *Industria*, formerly *Bodincomagus*, was abandoned during the V century. Regional (— • —) and municipal (— • • —) borders, centuriations (·····) and/or their orientations, and main roads, when known, are indicated as lines [Adapted from de Guillaume de Lisle (1715) *Tabula Italiae Antiquae in Regiones XI ab Augusto divisae* and Zanda, 2007, Zanda, 2011].

Accessibility of resources, including the procurement distances for soil as a raw material source, was carefully weighted in ancient societies (Schiffer and Skibo, 1997). Although in some cases, the distance travelled to reach a clay source was greater than 50 km, the exploited sources were usually available within a radius of 10 km from the brick-making site (Arnold, 1985). As an ideal raw terrigenous source for bricks does not exist, the soil employed in the brick-making had presumably to fit some criteria: a minimum content in clay (*i.e.* not lower than 20 percent by volume), a practical lack of soil skeleton, and a small amount of carbonates. Consequently, our selection of the potential sources of raw material for the ancient brick industry started with the scrutiny of soil composition maps related to the investigated area, made available by the Piedmont Region (Regione Piemonte, 2010). We selected soils and building samples from *Regio IX*, *XI* and *Alpes Cottiae*, in Italy and from *Regio Hispania Baetica* in Spain. Samples from Andalusia in the form of fired soils were extensively imported to ancient Italy by the Romans. The production of olive oil was transported in amphorae, and thousands of their debris are present in Italian settlements.

The straightforward identification of existing material sources in ancient times was not possible, because no open-pit had been discovered in the vicinity of the brick sampling areas. According to our hypothesis, the fluvial terraces most likely exploited in Roman times as clay sources could be identified by comparison of the chemical and physical properties between the main soil types of the region and the building materials located in the archaeological sites. In addition, it must be considered that since ancient times, the shorter the distance between the origin of raw materials for building (soil, water and wood for firing) and building sites (kilns and other constructions), the higher is the probability of matching.

In our study (Fig. 1), major soil sites have been located in Rovasenda and Vauda at North, Chieri at East, and Cellarengo and Poirino southeast of the former *Augusta Taurinorum* (Torino) and Piscina and Bagnolo along the southern part of the Piedmont plain; soil samples of Andalusia were from Bujalance and Aroche (Table 1). These soil sites have some characteristics of interest, namely: 1) the content of clay in their upper horizons is less than 25% in Poirino around 30–40% in Bene Vagienna, Tortona and Rovasenda, almost 40% in Bagnolo, Bujalance and Aroche, and less than 20% in Piscina, Vauda, Chieri and Cellarengo (a full description of the pedological features is available at www.regione.piemonte.it); 2) the ratio of sand particles, which is on average less than 30% of the total volume amount.

Table 1. Site data selected upon the localities of archaeological samples (✦ in Fig. 1).

Soil	Site	Coordinates	Former *Regio*	Soil Taxonomy[a]	Sequence of horizons	Clay	$CaCO_3$	Skeleton
						percent		
1	Poirino	44°5′N 7°51′E 177 m a.s.l.	IX *Liguria* (LI)	Typic Haplustalf	Ap-AB-Bt1-Bt2	>25	0	0
2	Piscina	44°55′N 7°26′E 288 m a.s.l.	*Alpes Cottiae* (CA)	Typic Hapludalf	Ap-Bt1-Bt2-BCt	>20	0	50[b]
3	Bagnolo	44°46′N 7°19′E 358 m a.s.l.	*Alpes Cottiae* (CA)	Typic Fraglossudalf	A-E-E/B-Btx	>40	0	0
5	Vauda	45°17′N 7°37′E 380 m a.s.l.	XI *Transpadana* (TP)	Typic Fragiudalf	A-E-Btx1-Btx2	>20	0	0
6	Chieri	44°59′N 7°52′E 276 m a.s.l.	IX *Liguria* (LI)	Inceptic Haplustalf	A-E/Bt-Bt1-Bt2	>20	0	0
8	Cellarengo	44°51′N 7°55′E	IX *Liguria* (LI)	Typic Haplustalf	Ap-E-Bt1-Bt2-	>20	0	0

Soil	Site	Coordinates	Former *Regio*	Soil Taxonomy[a]	Sequence of horizons	Clay	$CaCO_3$	Skeleton
						percent		
		320 m a.s.l.			Btg			
9	Rovasenda	45°32′N 8°19′E 220 m a.s.l.	XI *Transpadana* (TP)	Aquic Fraglossudalf	Ap-E-Btg1-Btg2- Btc	>30	0	0
10	Bujalance	37°53′N 4°23′W 357 m a.s.l.	*Hispania Baetica* (HB)	Vertic Xerochrepts	A-Bc-Bck	>40	>5	0
11	Aroche	37°56′N 6°57′W 420 m a.s.l.	*Hispania Baetica* (HB)	Calcic Haploxeralf	A-Bt-BCck	>40	>5	0
12	Bene Vagienna	44°33′N 7°50′W 350 m a.s.l.	IX *Liguria* (LI)	Typic Paleustalf	A-E-Bt-2Bt-3Bt	>30	0	0
13	Tortona	44°53′N 8°51′W 122 m a.s.l.	IX *Liguria* (LI)	Typic Haplustalf	Ap1-Ap2-Bt1-Bt2	>30	20[c]	0

[a] U.S. soil taxonomy (Soil Survey Staff, 1999) was used in surveys and mapping at the regional level. To facilitate the comparison we have decided neither to update nor to convert to other taxonomic systems. All soils are mixed, nonacid, mesic, their particle size distribution spans from fine-silty, fine-loamy, to loamy (URL www.regione.piemonte.it/agri/area_tecnico_scientifica/suoli/dati.htm).

[b] Below 150 cm.

[c] Below 120 cm.

All soil data related to B horizons are located at an average depth between 100 and 150 cm. All these soils do not contain stone lines or rock fragments, and due to their degree of pedogenesis, all of them are sub-acid or acid without carbonates in the upper horizons.

2.2. Materials

The rationale of these distributed samplings was to consider the largest amount of typologies of fired bricks and of the potential sites of raw materials available in the territory. Archaeological samples have been collected from public and private buildings with different uses (kiln, pipeline, wall) and constructive typologies (tiles and bricks) (Table 2). In one case, the stamp “M•A•[H]”, imprinted on the tile from Brandizzo, indicates probably the initials of the *figlina* owner, a local enterprise for the manufacture of bricks (Fig. 2).

Table 2. Archaeological bricks and tiles (✚ in Fig. 1).

Brick	Site	Coordinates	*Regio*	Site	Type	Epoch[a]
I	*Segusio*	45°8′N 7°3′E 503 m a.s.l.	*Alpes Cottiae* (CA)	*domus* – tile fall	Tile	I–III c. AD
II	*Segusio*	idem	*Alpes Cottiae* (CA)	*domus* – sporadic within the layer	Brick	I–III c. AD
III	Brandizzo	45°11′N 7°50′E 187 m a.s.l.	XI *Transpadana* (TP)	*villa rustica* – tile fall	Tile	I–II c. AD
IV	Brandizzo	idem	XI *Transpadana* (TP)	*villa rustica* – tile fall	Tile, stamp M·A·[H]	I–II c. AD
V	*Hasta*	44°53′N 8°12′E 123 m a.s.l.	IX *Liguria* (LI)	Brick (kiln?)	Brick	I–II c. AD
VI	*Hasta*	idem	IX *Liguria* (LI)	public building wall (positioning floor levelling course)	Brick	first half I c. AD
VII	*Hasta*	idem	IX *Liguria* (LI)	main sewer conduct under *decumanus*	Sewerage brick	I c. BC
VIII	*Hasta*	idem	IX *Liguria* (LI)	clay pipe conduct under *decumanus*	*Tubulus*	I–II c. AD

Brick	Site	Coordinates	*Regio*	Site	Type	Epoch[a]
IX	*Hasta*	idem	IX *Liguria* (LI)	clay pipe conduct under *decumanus*	*Tubulus*	I–II c. AD
X	*Vercellae*	45°19′N 8°25′E 130 m a.s.l.	XI *Transpadana* (TP)	amphitheatre foundation bedplate (outer ring)	Brick	II c. AD
XI	*Industria*	45°11′N 7°58′E 177 m a.s.l.	IX *Liguria* (LI)	Isis temple podium (levelling course)	Brick	I c. AD
XII	*Bujalance*	37°55′N 4°22′W 360 m a.s.l.	*Hispania Baetica* (HB)	Not determined	Tile	I c. AD
XIII	*Turóbriga*	37°58′N 6°56′W 270 m a.s.l.	*Hispania Baetica* (HB)	*thermae* – public baths	Tile (XIIa), brick (XIIb)	I c. AD
XIV	*Itálica*	37°26′N 6°02′W 18 m a.s.l.	*Hispania Baetica* (HB)	Not determined	Tile	II c. AD

[a] Dating (in centuries) have been made from the archaeological record by a direct study of artefacts deduced by association with other materials found in the context and inferred by their point of discovery in the sequence relative to datable contexts.

Fig. 2. a) Brandizzo (45°10′36.11″N 7°49′ 8.43″E, former *Regio Transpadana*), right bank of the river Bendola, Italy. Tiles and walls fall of a roman country house, *villa rustica* (archaeological tiles III and IV, ✚ in Fig. 1), consisting of a main building (54 by 60 m), two large courtyards, *cohortes*, around which there are stockrooms for food, small rooms of the residence of the tenants, gardens and fences for husbandry, *maceriae*. A few dozen of meters west from the main building a small square (side 12.5 m) could be a dryer for cereals, *fumarium*. The *villa* is positioned approximately in the middle of one of the four parts into which it is theoretically divisible a *centuria*, a hundred *heredia* or two hundred *jugera*, the common measure of land among the Romans (Barello, 2004), b) The stamp M•A•H is attributable to the owner of *figlina* (brickmaking local enterprise) or its conductor, in charge of management. M•A•H are probably the *tria nomina* initials, the Roman naming system, where M is the *praenomen* (given name of *Marcus*), A is the *nomen gentilicium* (family name: the possible name of the *gens* is virtually countless), H the *cognomen* (distinctive personal nickname, with many different alternatives). This stamp is presently known in the towns of *Industria* and *Augusta Taurinorum*, and in its surroundings, Settimo Torinese, Brandizzo (Nardi, 2011), c) M•A•H stamp on a tile incorporated within the NW wall of the main church in Monteu da Po, modern town by former *Industria*.

Furthermore, to verify the reliability of the results, some specimens were selected from other geographic areas culturally dependent from Rome whose soil fractions were similar to those previously considered, but having a different chemical fingerprint, as in the neighborhoods of the ancient cities *Augusta Bagiennorum* (Bene Vagienna, 44°32′43″N, 7°49′59″E) and *Julia Derthona* (Tortona, 44°53′39″N, 8°51′56″E), in Lomello and Oltrepò (soils) and Costeggio and Lomello (artefacts), and in the former Roman province of Spain, *Hispania Baetica* (geographically located at 37°25′N, 6°01′W) where two soils (Aroche and Bujalance) and three artefacts (Bujalance, Turobriga and Italica) were collected and compared. NIST 679 “brick clay” certified reference material was used to validate the experimental methodology for chemical analysis.

2.3. Chemical characterization

On the Earth's surface, trace elements are partitioned or separated (enriched or depleted) from each other during geological processes because of differences in their chemical properties. Geochemists use the relative concentrations of trace elements to infer the chemical conditions under which a rock was formed. Specifically, relative enrichments of rare earth elements (REE: La, Ce, Pr, Nd, Sm, Eu, Gd, Tb, Dy, Ho, Er, Tm, Yb, and Lu) are difficult to appreciate as their abundance in soils is scattered. However, REE elements

always occur together: as a consequence their local differentiation through mobilization and redistribution processes, which can result in fractionation of elements that can be used as tracers of pedogenetic transformations, the latter being extremely long-term processes (Nesbitt, 1979, Braun et al., 1993). REE patterns, at least for a few decades yet (Alonso et al., 2012), may shed some light on past human activity involving soil use (Saiano and Scalenghe, 2009, Gliozzo, 2013). REY (REE plus yttrium) concentrations are usually normalized with respect to different geochemical references. The Upper Continental Crust (UCC) was chosen as reference, which has long been the standard for geochemical investigations (Wedepohl, 1995).

To exploit the selective approach in the procedure aimed at inferring provenance through chemical analysis, based on the similarity of the chemical and physical properties of the REY, a feature able to explain their widespread occurrence as a group and their common behavior in the environment (Henderson, 1984), ICP-MS instrumental technique was used to investigate the distribution of REY. All chemicals used for the preparation of ICP-MS samples were of ultrapure grade or higher when available, and all solutions were prepared with ultrapure water at 18.2 MΩ cm obtained by a Thermo EASYpureII purification system. Working standard solutions for each element were prepared through successive dilution of BDH, Merck or CPI International, 1000 ± 5 μg mL^{-1} elemental standard solution in a HNO_3 1 mol L^{-1} medium. Laboratory equipments were polyethylene, polypropylene, or Teflon. Determination of trace and minor elements was performed on solutions obtained by microwave digestion of 250 mg of sample with HNO_3, HF, and HCl 3:1:1 (EPA Method 3052). The investigated elements were determined using an Agilent 7500ce ICP-MS spectrometer equipped with a collision cell. Rhodium solution (1 ng mL^{-1}) was used as internal standard. Validation of the whole procedure (sample preparation and quantitative measurement) was carried out using certified “light sandy soil” reference material (EU Bureau of Reference CRM142R/419). Experimental standard deviation, evaluated by replicate analyses, is in the range of ±10% for all the investigated elements.

2.4. Mineralogical characterization

X-ray diffraction (XRD) and infrared spectroscopy (IR), were used because of the effectiveness of these techniques to differentiate ceramic samples, as demonstrated in previous studies (Weckler and Lutz, 1998), focusing on the mineralogical transformation of the clayey matrix upon heating. XRD measurements were performed on powdered fine-earth samples using a Bruker D8 Advance diffractometer (CuKα, 40 kV, 40 mA, antiscatter slit 0.115° 2θ, soller slits 2.5° 2θ) equipped with a LynxEye detector. Sample investigations were recorded in scanning mode and converted to angular patterns (step 0.025°) from 2.5 to 65° (2θ configuration) using 0.6 s or 1.2 s counting time per step. IR measurements were performed on KBr pellets prepared from a mixture of 150 mg of dry KBr and 1.5 mg of dried powder (soil or brick) and analysed on a Nicolet 760 FTIR spectrometer. Spectra displaying the OH-stretching bands (3000–3800 cm^{-1}) were acquired after drying the pellet for one day at 105 °C. In the near infrared region, undisturbed samples were analysed using a Nicolet 6700 spectrometer with a wavenumber resolution of 4 cm^{-1} using a NIR DRIFT accessory from SpectraTech.

2.5. Magnetic characterization

In addition to the previously described investigation techniques, magnetisation curves were measured on selected samples to appreciate their magnetic features and follow the evolution of the magnetic properties after thermal treatments. Clay minerals usually contain iron as a minor element, whose total content rarely is above 5% and is almost entirely converted into pedogenic Fe oxides that give the ferromagnetic properties to the clay matrix. Magnetic measurements are able to illustrate the structural changes taking place when clay is heated (La Borgne, 1965, Caitcheon, 1993, Yang et al., 1993, Dalan and Banerjee, 1998, Hus et al., 2002). The oldest literature available for the magnetic properties of ancient ceramics consists of an ensemble of experimental works analysing the technological circumstances under which pottery samples were prepared. Pioneering works of Bouchez et al. (1974) and Coey et al. (1979) examined the effects of temperature and

reducing atmosphere during thermal treatments on the magnetic properties of iron oxides embedded within ceramic bodies. The determination of firing temperatures was mainly investigated by differential thermal analysis, thermal expansion measurements, and Mossbauer spectrometry. Magnetic techniques were applied to study the processing of clays and firing conditions of pottery (Coey et al., 1979, Maggetti and Schwab, 1982, Tema, 2009). After Van Klinken (2001), who tried to order phase transformations and magnetic properties of iron oxides particles, attention was then mainly focused onto archaeomagnetic dating of ceramics (Fouzai et al., 2012).

For our experiments, the magnetisation curves of tiles and bricks (fragments of mass ~50 mg) were measured on the samples as found, using a Vibrating Sample Magnetometer Vector 7410 Lakeshore (maximum applied field H_M = 1000 mT). Measurements were repeated on different portions of all the samples and the values of the resulting parameters averaged. As the magnetic behaviour of the samples as found can hardly be attributed directly to the source of the soil used for their production, annealing sequences were applied on selected soil and ceramic samples and the magnetic parameters – such as the coercive field (H_c) and remanence (M_R) – were extracted from the hysteresis cycles and analysed as a function of the applied temperature. This approach has been applied as the subsequent thermal treatments permits reconstruction of the sequence of changing magnetic properties with temperature, which is a specific characteristic of soils that is still recognizable in artefacts. Thermal treatments were carried out in subsequent 100 C° steps, from room temperature up to 900 °C. Heating was directly applied in the VSM using a thermal-resistance set-up along with a constant field H = 100 mT applied to the sample. Saturation magnetisation (M_S) was calculated after graphic subtraction of the non-ferrimagnetic contributions. Remanence (M_R) corresponds to the magnetisation retained by the sample after the H_M field is released. Comparison of the magnetic properties was made at the end of the annealing sequences. Magnetic similarities between samples and clays after thermal treatments can, eventually, be used to appreciate the technological conditions applied for production, such as temperature, atmosphere, and duration of firing (Beatrice et al., 2008).

2.6. Speculation on brick-making technology

In order to provide hypotheses on the provenance of ceramics on the basis of technological and archaeological analogies, experimental replicates of past brick-making technology were used to prepare clay briquettes with volumes about 50 cm^3 (8 × 4 × 1.5 cm; Wolf, 2002). In addition, cubes of approximately 5 cm^3 were dried at 60 °C for one day, and then fired in an electric furnace under oxidising atmosphere at a final temperature of 750 °C for 14 h (T ramp ~150 °C h^{-1}). The small cubes were made of soil mixed with deionised water and showed various hues, from yellow to reddish according to the main colour of the parent soil. As in ancient furnaces, only a few cubes directly adjacent to the chimney conveyor, where the temperature is higher, vitrified or cracked while experiencing high temperatures, T > 900 °C (Wolf, 2002). As, in general, the majority of bricks experienced temperatures higher than 600 °C, we estimated for a single kiln load replica experiment an average temperature equal to 750 °C.

In addition, a replica drying experiment was performed with the aim of evaluating the operability of the brick-making process. Sesquipedalian bricks (45 × 30 × 10 cm) were formed in wooden boxes without bases, using all the soils sampled matching the ancient *Regio IX*, *XI* and *Alpes Cottiae* (*i.e.* excluding soils sampled for comparison). A variable volume of water was added to reach the optimal workability of each soil mixture. Then, individual freshly cast bricks were compacted manually and placed on a wooden base insulated from the ground by a sand film, to dry by natural processes for up to three months (Fig. 3a).

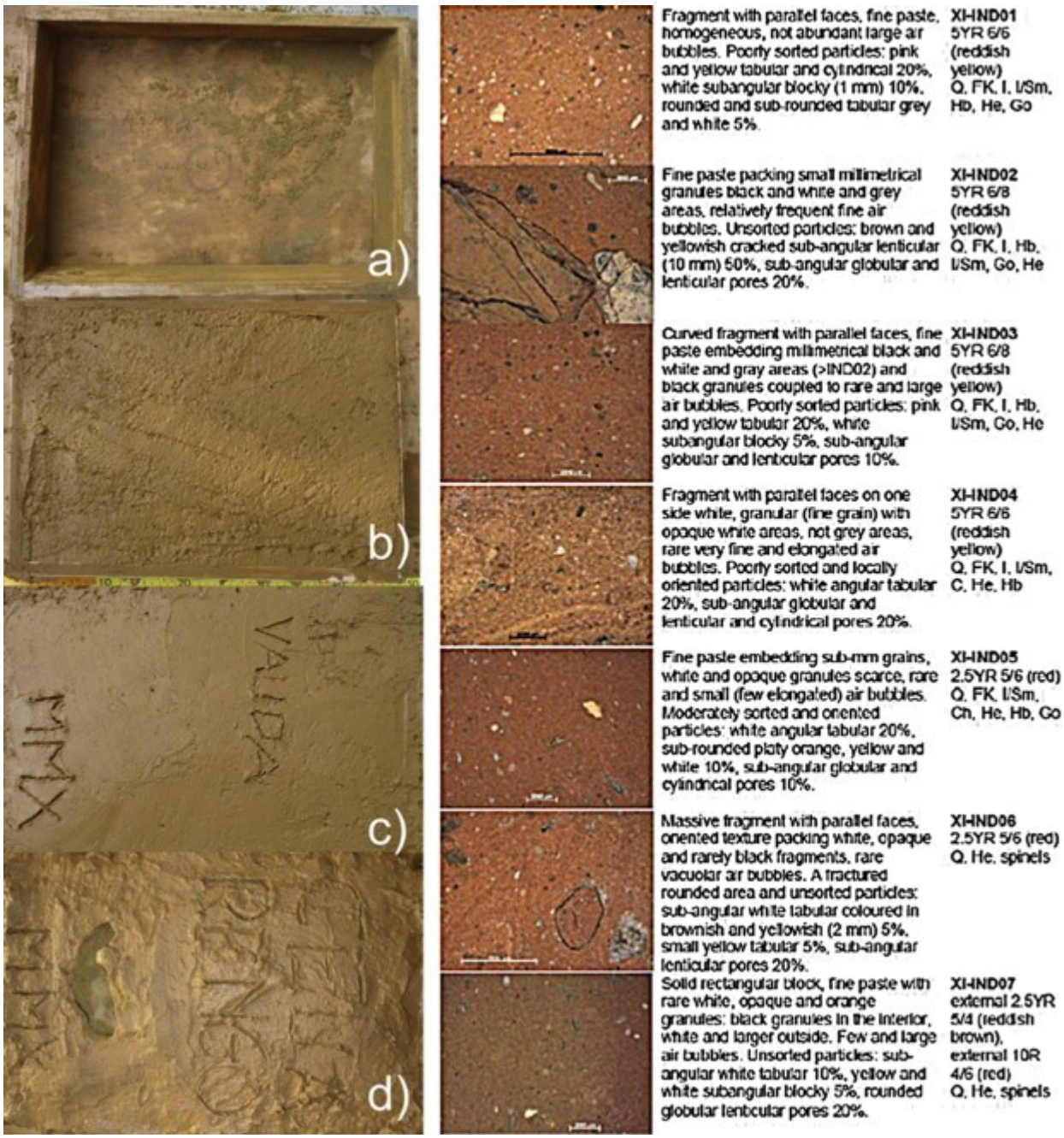

Fig. 3. **a)** Replica brickmaking of sesquipedalian bricks (45 × 30 × 10 cm) were formed in a) wooden boxes without bases, b) using all the soils, c) individual freshly cast brick was placed on a wood base insulated from the ground by a sand film, d) to dry for up to three months. **b)** Optical microscopy micrographs of seven bricks sampled in the site XI-*Industria* (45°09′32.98″N 8°01′08.25″E, 170 m a.s.l.) [samples have been sawed in dried conditions, one face was successively polished on abrasive disks of 10, 5 and 1 μm size-grain].

3. Results

3.1. Provenance of raw material for brick-making

In an attempt to identify any objective parameter differentiating artefacts and soils of different sources as well as any link between artefacts and soil sources, attention was addressed to REY elements. In all samples, in terms of concentrations, cerium, lanthanum, neodymium, and yttrium account for more than 80% of all the REYs (Table 3, Table 4) with a nearly symmetrical and platykurtic general distribution (skewness <0.4, kurtosis −1.7/−0.4). A close examination of the REY data allows the identification of some parameters that can be used for discrimination purposes, to find differences or similarities between artefacts and soils, or for

provenance assignment of the artefacts themselves. The relationships between the rare earth elements are often used to highlight different behaviours between the light and heavy REY. Therefore, we have calculated the $(\Sigma LREY/\Sigma HREY)_{UCC}$ (*i.e.* the ratio between the content of light REY (from La to Eu) and the content of heavy REY (from Gd to Lu plus Y)) and the $(Gd/La)_{UCC}$ molar ratio. In the lower part of Table 3, Table 4, the values for these parameters are reported for both soils and artefacts.

Table 3. REY in soils fired at 60°C, in the vicinities of the localities of archaeological samples. Unit: μmol kg^{-1}.

	1	**2**	**3**	**5**	**6**	**8**	**9**	**10**	**11**	**12**	**13**
	Poirino	**Piscina**	**Bagnolo**	**Vauda**	**Chieri**	**Cellarengo**	**Rovasenda**	**Bujalance**	**Aroche**	**Bene Vagienna**	**Tortona**
Y	92	61	71	93	94	101	55	76	81	185	133
La	98	44	81	100	117	128	55	85	35	276	224
Ce	205	105	205	206	239	262	128	179	100	602	432
Pr	24.0	13.2	21.9	24.6	29.5	31.5	15.3	20.9	12.0	66.1	57.9
Nd	92	53	86	95	114	121	60	76	47	216	199
Sm	18.8	11.3	17.3	18.5	22.2	23.9	12.5	11.7	8.5	40.0	38.9
Eu	3.9	2.2	3.2	3.6	3.7	4.2	2.4	2.5	2.5	6.8	6.4
Gd	16.8	10.4	15.1	16.6	18.5	20.4	11.1	10.9	9.0	47.7	43.1
Tb	2.3	1.6	2.1	2.2	2.5	2.7	1.6	1.2	1.3	4.2	3.5
Dy	12.3	9.5	11.1	12.0	12.5	13.5	8.9	6.3	7.7	20.0	15.9
Ho	2.2	1.9	2.0	2.2	2.2	2.4	1.6	1.1	1.5	3.4	2.6
Er	6.3	5.6	5.8	6.2	6.1	6.7	4.8	2.9	4.3	8.6	6.6
Tm	0.9	0.8	0.8	0.9	0.8	0.9	0.7	0.4	0.6	1.1	0.9
Yb	5.5	5.6	5.2	5.4	5.5	5.9	4.7	2.3	3.8	6.7	5.6
Lu	0.8	0.9	0.8	0.8	0.8	0.9	0.7	0.3	0.5	0.7	0.6
$\Sigma LREE_{UCC}$	5.9	3.4	5.4	5.9	6.9	7.5	3.8	4.1	2.8	14.1	12.8
$\Sigma HREE_{UCC}$	4.2	3.5	3.8	4.1	4.2	4.6	3.2	2.1	2.8	6.3	5.0
$(Gd/La)_{UCC}$	1.5	2.1	1.7	1.5	1.4	1.4	1.8	1.1	2.3	1.5	1.7

Table 4. REY in archaelogical bricks and tiles. Unit: μmol kg^{-1}.

I	**II**	**III**	**IV**	**V**	**VI**	**VII**	**VIII**	**IX**	**X**	**XI**	**XII**	**XIII**	**XVI**
Segusio	***Segusio***	**Brandizzo**	**Brandizzo**	***Hasta***	***Hasta***	***Hasta***	***Hasta***	***Hasta***	***Vercellae***	***Industria***	***Bujalance***	***Turòbriga***	***Itàlica***
160	141	194	211	99	234	210	141	122	210	208	75	78	53
132	178	155	184	100	237	185	137	125	187	177	72	33	45
269	355	334	382	207	466	371	278	257	385	363	158	88	109
32.6	40.8	38.5	44.0	24.8	54.8	44.0	34.1	30.6	44.8	43.2	19.0	11.4	13.1
125	154	150	170	96	208	168	132	118	172	167	69	45	48
26.8	29.1	31.5	35.3	19.3	41.1	34.4	27.0	23.8	34.9	34.0	10.7	8.1	7.3
4.6	5.9	6.4	7.1	3.7	7.7	7.0	5.4	4.0	7.9	6.9	2.2	2.3	1.4
24.4	25.4	29.1	32.8	17.5	37.4	32.0	24.9	21.6	31.7	31.3	9.9	8.6	6.9
3.6	3.4	4.2	4.6	2.5	5.1	4.5	3.5	3.0	4.5	4.5	1.1	1.2	0.8
19.3	17.5	23.6	25.3	13.6	27.1	24.8	19.0	16.0	24.7	24.7	6.0	7.3	4.2

I	II	III	IV	V	VI	VII	VIII	IX	X	XI	XII	XIII	XVI
Segusio	***Segusio***	**Brandizzo**	**Brandizzo**	***Hasta***	***Hasta***	***Hasta***	***Hasta***	***Hasta***	***Vercellae***	***Industria***	***Bujalance***	***Turòbriga***	***Itàlica***
3.5	3.1	4.4	4.7	2.5	4.8	4.6	3.5	2.9	4.6	4.6	1.1	1.4	0.8
9.9	8.6	12.5	13.2	7.1	13.3	12.7	9.8	8.2	13.1	12.9	2.9	4.1	2.1
1.4	1.1	1.7	1.8	1.0	1.8	1.7	1.3	1.1	1.8	1.8	0.4	0.6	0.3
8.9	7.0	10.7	11.4	6.2	10.6	10.7	8.2	7.0	11.3	10.8	2.4	3.7	1.9
1.3	1.0	1.6	1.7	0.9	1.5	1.6	1.2	1.0	1.7	1.6	0.3	0.5	0.2
8.2	9.4	9.8	11.1	6.1	13.1	10.9	8.4	7.5	11.0	10.7	3.7	2.6	2.5
6.7	5.8	8.2	8.8	4.6	9.0	8.5	6.4	5.4	8.7	8.5	2.1	2.7	1.5
1.6	1.3	1.7	1.6	1.6	1.4	1.5	1.6	1.5	1.5	1.6	1.2	2.3	1.4

In particular, considering the $(Gd/La)_{UCC}$ ratio shown in Fig. 4, we reported for comparison four different Italian soils and two artifacts of the neighbouring regions (BeneVagienna, Tortona, Lomello and Oltrepò soils and Costeggio and Lomello artefacts), two Spanish soils (Aroche and Bujalance) and three Spanish artefacts (Bujalance, Turobriga and Italica) and a NIST CRM 679 “brick clay”. To obtain information correlating soils with bricks, preliminarily the element abundances in the raw and fired soil samples were compared to verify the conservative role of REYs subjected to the brick-making process. The REY concentrations in the fired samples are on average higher than in the raw ones. The concentration variations appear to be closely related to the mass loss upon firing and the differences in loss on ignition are related to the different content of carbonaceous rock and clay minerals. The REY element concentrations for raw *vs.* fired soil samples (data not shown) are strongly correlated with a R^2 higher than 0.996. This means that no information on the correlation among the investigated elements is lost during firing and that the raw sample element abundances can be safely used for archaeometric purposes. As can be observed (Fig. 4), soils and artefacts are distributed in groups suggesting the same regional provenance. Along with results in Fig. 5 and Table 3, Table 4, these results suggest a similarity in terms of $\Sigma LREY_{UCC}$, $\Sigma HREY_{UCC}$ and $(Gd/La)_{UCC}$ ratio of the Piedmont soil samples and artefacts as well as a difference with respect to the Spanish samples. The clear but not so trivially predictable differences with soil and artefacts of the neighboring Piedmont regions were interesting. The large overlapping of soils and artefacts in the $(Gd/La)_{UCC}$ ratio graph did not indicate a direct link between artefacts and potential soil sources. The differences relating to the concentrations of Gd and La, which is higher in artefacts than in soils, are due to the loss of organic substance and carbonates at high temperatures (600–900 °C) when firing is applied to make the artefacts themselves. However, the $\Sigma LREY/\Sigma HREY$ and $(Gd/La)_{UCC}$ ratios do not reveal all the information available on the distribution of the fifteen REY elements studied. For example, because the REY_{UCC} normalized pattern represents a sample fingerprint, its use as a reference to compare similarities or differences of soil and artefact patterns, could support correlation of the artefacts with their possible soil sources.

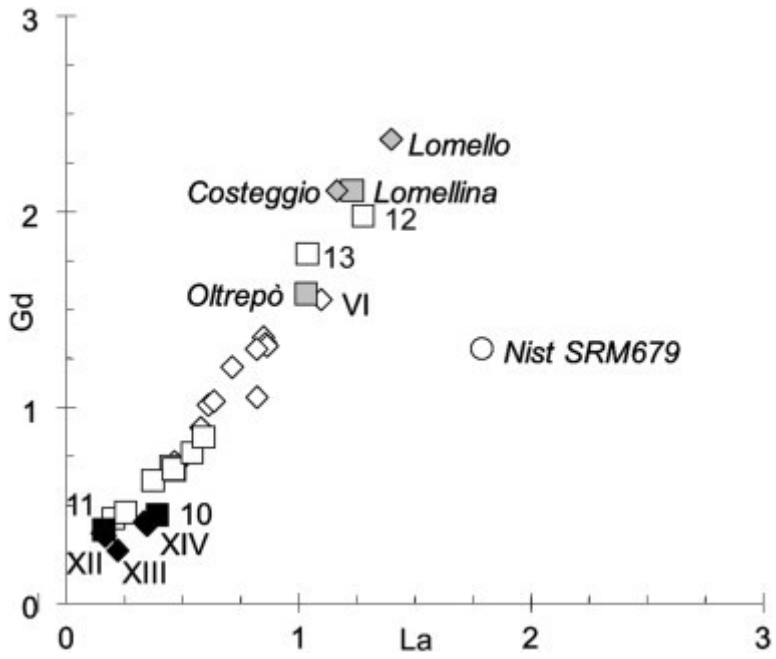

Fig. 4. Gadolinium *vs*. lanthanum (μmol kg^{-1}). Diamonds indicate bricks; squares indicate soils. Data from Meloni et al. (2000) in italics (gray symbols). Filled symbols refer to Andalusian materials and soils from the former Imperial Roman province *Hispania Baetica*; circle is a reference "brick clay" material.

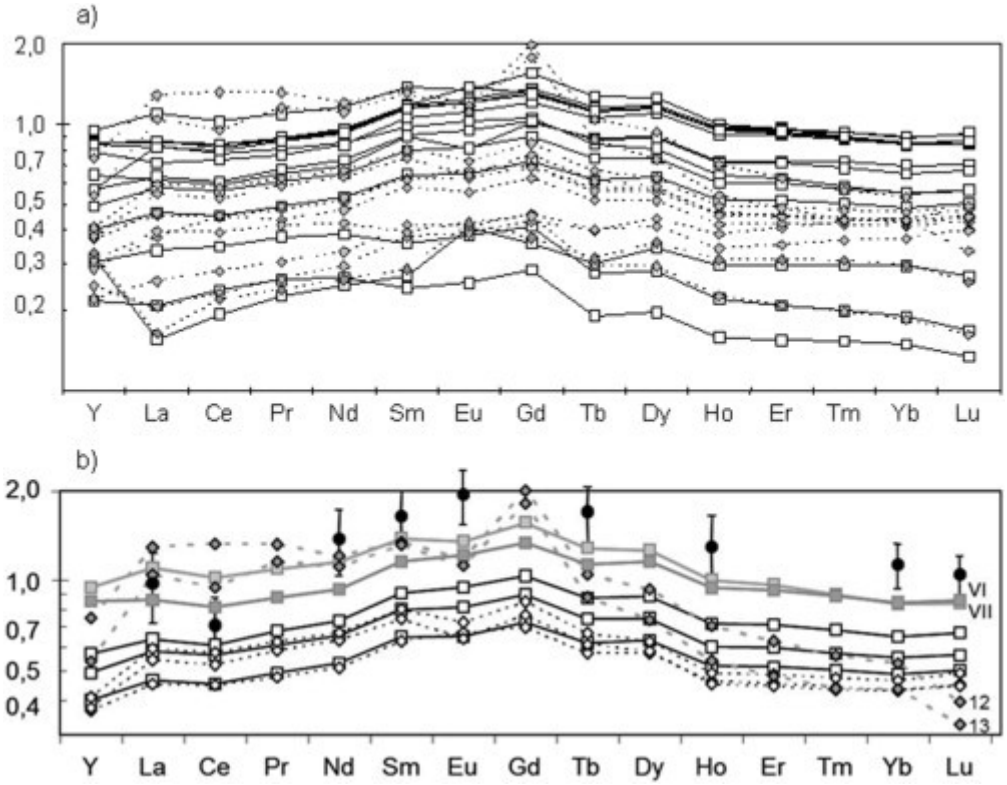

Fig. 5. **a)** REY_{UCC} pattern for all samples analyzed. Normalized diagram arranged following the periodic table by group. In ordinates REY_{sample}/REY_{UCC}. Diamonds and dotted lines indicate bricks while squares and solid lines indicate soils. **b)** REY_{UCC} pattern for all samples from Hasta and soils (1, 6 and 8) in the neighborhood of 50 km. Archaeological samples VI and VII in grey; filled symbols indicate the medians ±SD of REY of Cenozoic clays *Regio VI Umbria* (Bottaccione near Gubbio 43°21′N 12°34′E).

In Fig. 5a, the REY_{UCC} patterns are shown for all the samples analyzed. In Fig. 5b, the case of five fragments (V–IX) from *Hasta* is presented: three of them (V, VIII, IX) show overlapping of their REY patterns with the soils in their vicinity. This is assumed to be geochemical evidence of the origin of the raw material utilized in their brick-making. Brick VI from the positioning floor of a public building and brick VII

from the main sewer conduit under *decumanus* differ slightly. Their patterns show also similarities with the REY pattern of clays from *Regio VI Umbria* (Bottaccione near Gubbio 43°21′N 12°34′E, data from Ebihara and Miura, 1996). This fact may open several plausible interpretations, from mixing of the raw material to the long distance transportation of special bricks (*e.g.* for final use or due to their technological characteristic as a sewer conduit). However, these two bricks have not been made using only local soils. The soil of Piscina was the only one of the examination group whose REY_{UCC} pattern did not match any of the considered artefacts.

Our results are consistent when superimposed on the map reporting the $(Gd/La)_{UCC}$ ratio distribution in the analyzed region (Fig. 6). With this map it is possible to discriminate chemical signatures and individual soil and brick samples of Piedmont from those having other geological and archaeological origins. The $(Gd/La)_{UCC}$ ratio also differentiates the inter-site chemical signatures, suggesting possible soil sources for different artefacts.

Fig. 6. $(Gd/La)_{UCC}$ ratio. Thin crosses indicate a measured Gd/La ratio in Roman bricks while bulky crosses indicate the same ratio in soils. Dotted lines are iso-ratio lines of independent measures (ARPA Piemonte data; Biasioli et al., 2012) from A, B and C soil horizons [aqua regia extracts analysed with Agilent 7500ce ICP-MS, contour maps from ordinary Kriging, linear model, nugget 0.02, direction −55; N = 534].

A thorough analysis of data and REY_{UCC} patterns suggested the relations reported in Table 5. The best artefacts-soils matching available in the explored range was in all cases indicative of local exploitation: the source of raw material matching the REY pattern of bricks is likely to be located within the limits of one-day terrestrial transport, *i.e.* an area with a radius between 40 and 70 km. In general, on the basis of a quite large grid of observations, it is possible to guess an intra-*Regio* utilisation of soil as material resource for the local brick industry, except for samples I and II, a tile and a brick respectively, imported from elsewhere. This supposition is supported, in the former case, by the small dimensions of the sample (which favours transportability) and for both cases by their discovery in a clay-poor area.

Table 5. Matching table. Roman bricks *vs.* most probable soils utilised as raw material based on the REY_{UCC} pattern. Matching shown only matches where their individual probability is associated with a two-tailed heteroscedastic Student *t* test >0.58, if the most probable distance by Roman roads was <100 km.

Archaeological artefact	Raw soil
I-*Segusio*	3-Bagnolo 6-Chieri 8-Cellarengo 9-Rovasenda
II-*Segusio*	1-Poirino
III-Brandizzo IV-Brandizzo V-*Hasta* VIII-*Hasta* IX-*Hasta* XI-*Industria*	5-Vauda
X-*Vercellae*	1-Poirino 3-Bagnolo 5-Vauda

3.2. Mineralogical characterization

Quartz is the main component of bricks (Fig. 3b). It has an angular shape of varying size, from a few micrometers to several millimeters. This mineral is a natural component of the sediments in the Po River basin, and it is commonly found in similar-sized grains in the soils. This indicates that quartz fragments occurred in the clay matrix. Technological analogies have been assumed from tempera of the ceramic pieces found in the Roman city of *Basti* (Cultrone et al., 2011). Apart from quartz, which prevails in all bricks and tiles, the other major components are either plagioclases or K-feldspars. Hornblende, illite, and paragonite-like clay minerals also occur in some samples. Goethite appears in traces in the first two bricks from *Segusio*, while hematite occurs in all samples. Calcite occurs in Andalusian samples only. Mullite does not occur in any sample (Table 6). Soils assumed to be potential sources of raw material for brick-making are always rich in quartz followed by plagioclases, but K-feldspars are not very abundant and often absent. The most common 2:1 phyllosicates are chlorites, muscovite-like and paragonite-like minerals. Although chlorite is generally the most abundant of these phases, it is not observed in the three Andalusian soil samples containing carbonates (calcite mainly). Iron oxides as goethite appears in traces in two soils from Vauda and Chieri while hematite does not seem to occur. The soil of Tortona is the only one showing vermiculite and swelling minerals (smectite) as phyllosicate phases.

Table 6. XRD bricks and tiles.

Artefact		Colour[a]	Q[b]	FK	P	Hb	V	Sm	Ch	M1	M2	I	Ho	Go	He	Ca	Do	Ge	Py	Mu
I	*Segusio*	5YR 7/4	++ +	++	+	(+)				+				(+)	+					
II	*Segusio*	5YR 6/6	++ +	+	+ +									+	++					
III	Brandizzo	2.5YR 6/8	++ +		+ +	(+)									++					
IV	Brandizzo	5YR 6/8	++ +	+	+	+									+					
V	*Hasta*	5YR 6/6	++ +	+	+					+					+					
VI	*Hasta*	5YR 8/6 5YR 8/3	++ +	++	+										+	+	(+)		(+)	
VII	*Hasta*	7.5YR 8/6 7.5YR 7/6	++ +	+	+										+	(+)				

Artefact		Colour[a]	Q[b]	FK	P	Hb	V	Sm	Ch	M1	M2	I	Ho	Go	He	Ca	Do	Ge	Py	Mu
VIII	*Hasta*	2.5YR 4/4	++++	+	+	(+)				(+)		(+)			+					
IX	*Hasta*	2.5YR 5/4	++++	+	+										++					
X	*Vercellae*	10R 5/8	++++	++	+	+				+					+					
XI	*Industria*	5YR 6/6	++++	+	+	+									+					
XII	*Bujalance*	2.5YR 8/4	++++	(+)	(++)										(+)	++		+		
XIII	*Turóbriga*	7.5YR 4/6	++++	(+)	(++)					+					(+)	++				
XIV	*Itálica*	7.55YR 7/8	++++	(+)	(++)					(+)					(+)	++				

[a] Colour zoning from the rim towards the center of the brick or tile.

[b] Q (quartz), FK (K-feldspath), P (plagioclase), Hb (amphibole), V (vermiculite), Sm (smectite), Ch (chlorite), M1 (muscovite-like), M2 (paragonite-like), I (illite), Ho (hornblende), Go (goethite), He (hematite), Ca (calcite), Do (dolomite), Ge (gehlenite), Py (pyroxene), Mu (mullite). In parenthesis poorly crystalline phases, bold high crystallinity.

In general, the possible sources of raw materials match with the qualitative mineralogy of the Roman artefacts. This is well exemplified for a sesquipedalian brick when compared with the soil horizon in which it has been discovered (Fig. 7a). However, the mineralogy of crude soils and bricks differs at least partially (Table 7): thermal effects due to firing affect the initial mineralogy.

Table 7. XRD unfired soils.

Soil		Q[a]	FK	P	Hb	V	Sm	Ch	M1	M2	I	Ho	Go	He	Ca	Do	Ge	Py	Mu
1	Poirino	+++	+	++				++	+	+									
2	Piscina	+++	+	++				++	+	+									
3	Bagnolo	+++	+	+				++	+	+									
5	Vauda	+++		++			(+)	++	+	+	(+)		(+)						
6	Chieri	+++		++				+	+	+		+	+						
8	Cellarengo	+++		++				+	+	+									
9	Rovasenda	+++		++				++	+	+									
10	Bujalance	+++					(+)		+						++	+			
11	Aroche	+++							+	+					+				
12	Bene Vagienna	+++	+	++	+		(+)	+	+	+	(+)								
13	Tortona	+++	+		+	(+)	+												

[a] Q (quartz), FK (K-feldspath), P (plagioclase), Hb (amphibole), V (vermiculite), Sm (smectite), Ch (chlorite), M1 (muscovite-like), M2 (paragonite-like), I (illite), Ho (hornblende), Go (goethite), He (hematite), Ca (calcite), Do (dolomite), Ge (gehlenite), Py (pyroxene), Mu (mullite). In parenthesis poorly crystalline phases, bold high crystallinity.

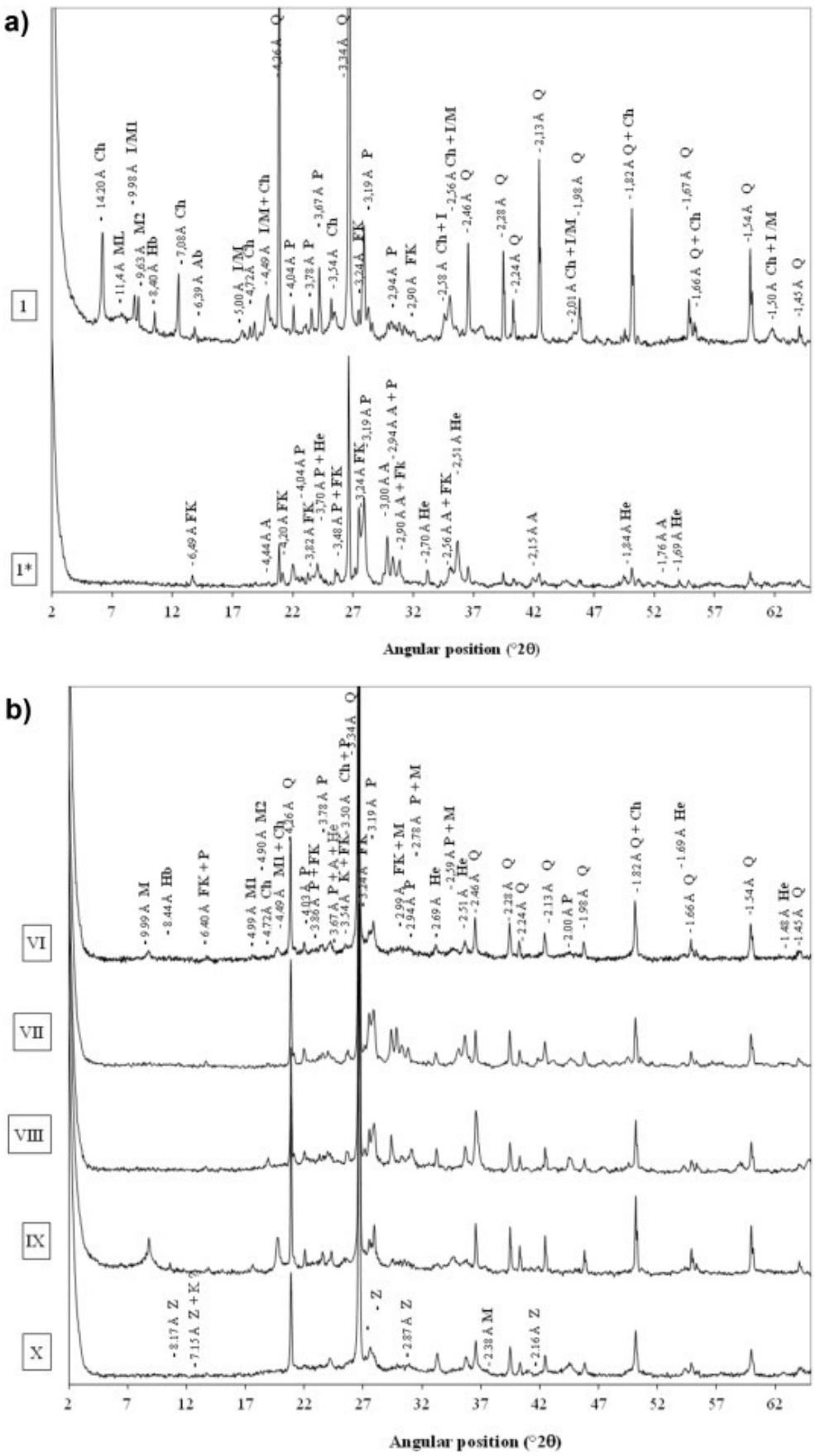

Fig. 7. a) Comparison of X-ray powder diffraction patterns of Poirino soil (1) and a sesquipedalian brick from Cava Carena (44°58’55”N 07°47’25”E) in Poirino (1*). The mineral phases identified are: chlorite (Ch), mixed-layer (ML), illite or mica 1 (I/M1), mica 2 (M2), quartz (Q), feldspar K (FK), plagioclase (P), hematite (He) and augite (A). **b)** Patterns of X-ray diffraction powders of five samples of bricks. The mineral phases identified are mica (M), amphibole (Hb), zeolite-like (Z), quartz (Q), feldspar K (FK), plagioclase (P), goethite (Go), and hematite (He).

3.3. Magnetic characterization

Fig. 8 shows the distribution of soils and ceramic fragments according to their magnetic (M_R *vs.* H_c) characteristics, as attained by VSM measurements of the magnetization curves at room temperatures. The analysis of magnetization curves is useful for a qualitative evaluation of the magnetic character of the samples. High field slopes of magnetization curves indicate paramagnetic contributions, which can be of paramount importance in ceramic materials fired at low temperatures. Tight loops indicate the presence of a single phase contributing to magnetic coercivity (Atkinson and King, 2005). Samples consisting of multiple magnetic fractions – usually a combination of ferrimagnetic (magnetite, maghemite) and anti-ferromagnetic (hematite, goethite) minerals – show open distorted loops. On the basis of their stable (*i.e.* high M_R, high H_C, large or distorted loops indicating a prevalence of antiferromagnetic particles) or unstable magnetic behaviour (*i.e.* low M_R, low H_C, linear-reversible loops indicating an important paramagnetic and/or superparamagnetic contribution by smaller iron-oxide particles), samples can be classified into three different groups: 1) magnetically stable ceramics retaining low slope at high fields, tight loops, and high remnant magnetization (only represented by sample VII); 2) less magnetically stable samples, which combine distorted loops with relatively high remnant magnetization (*e.g.* most of the ceramics along with soils 11 and 12); and 3) soil samples, plus ceramics VIII and X, exhibiting unstable magnetic properties, characterized by linear-reversible loops, low remnant magnetization, and high slope at high fields.

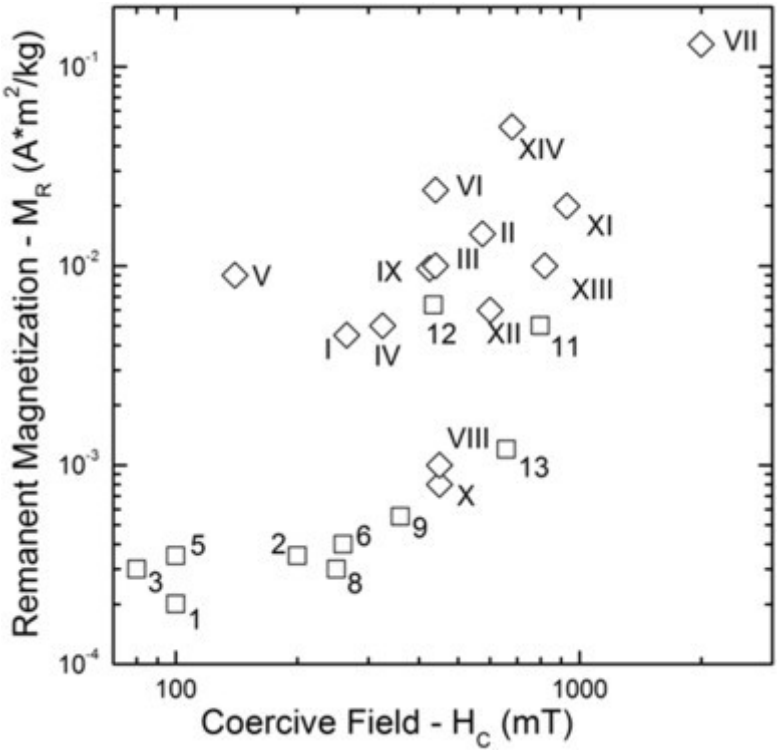

Fig. 8. Distribution of remnant magnetization – M_R *vs.* coercive field – H_C (M_R *vs.* H_C). M_R is the remnant magnetization value after applied field H_{max} up to 300 mT; H_C is the corresponding coercive field.

3.3.1. Variable-temperature magnetic measurements

The magnetic properties of ancient bricks and tiles have been used also to evaluate the technological conditions applied for their production: temperature, atmosphere, and duration of firing (Beatrice et al., 2008, Mirti et al., 1990). In our case, the magnetic behaviour of the samples as found can hardly be related to the source of soil used for their production. Therefore, annealing sequences were applied in the temperature range from 400 °C to 900 °C, following the magnetic moment variation (constant applied field H_{max} = 3

kO_e), while the usual magnetic parameters, such as the coercive field (H_c, mT) and remnant magnetization (M_R, $Am^2\ kg^{-1}$) were obtained from hysteresis cycles measured after each thermal treatment.

As an example, in Fig. 9 the change of magnetic properties with temperature of a tile and a soil, both collected in Andalusia, within a distance of few kilometres, are reported. In Fig. 9a, the magnetic loops measured are compared, showing a similarity of the tile XIII with respect to the clay 11 sample. Because magnetic properties vary when thermal treatments are applied at increasing temperature, the correspondence between the two specimens is rather confidently established if the whole plot of the magnetic behaviour with temperature is examined (Fig. 9b). Experimental results indicate a close relationship, as evidenced by the common magnetic patterns of the tile (dashed line) and clay (continuous line) samples in the temperature range from 600 °C to 800 °C. Furthermore, since tile XIII consistently modifies its properties only after experimental heating at 700 °C, it is supposed to have experienced an equivalent temperature treatment in the past between 600 °C and 700 °C. The overlapping of the hysteresis cycles measured on the samples after thermal treatments above 600 °C (Fig. 9c) confirms the closeness of the magnetic properties of the soil and artefact. A final comparison is made reporting the thermomagnetic curves of both samples, previously treated at 700 °C, up to 800 °C (Fig. 9d). Similarities are observable in the curve shapes, having two Curie temperature points corresponding, respectively, to titano-magnetite (T_C ~ 550 °C) and titano-hematite (T_C ~ 700 °C) minerals.

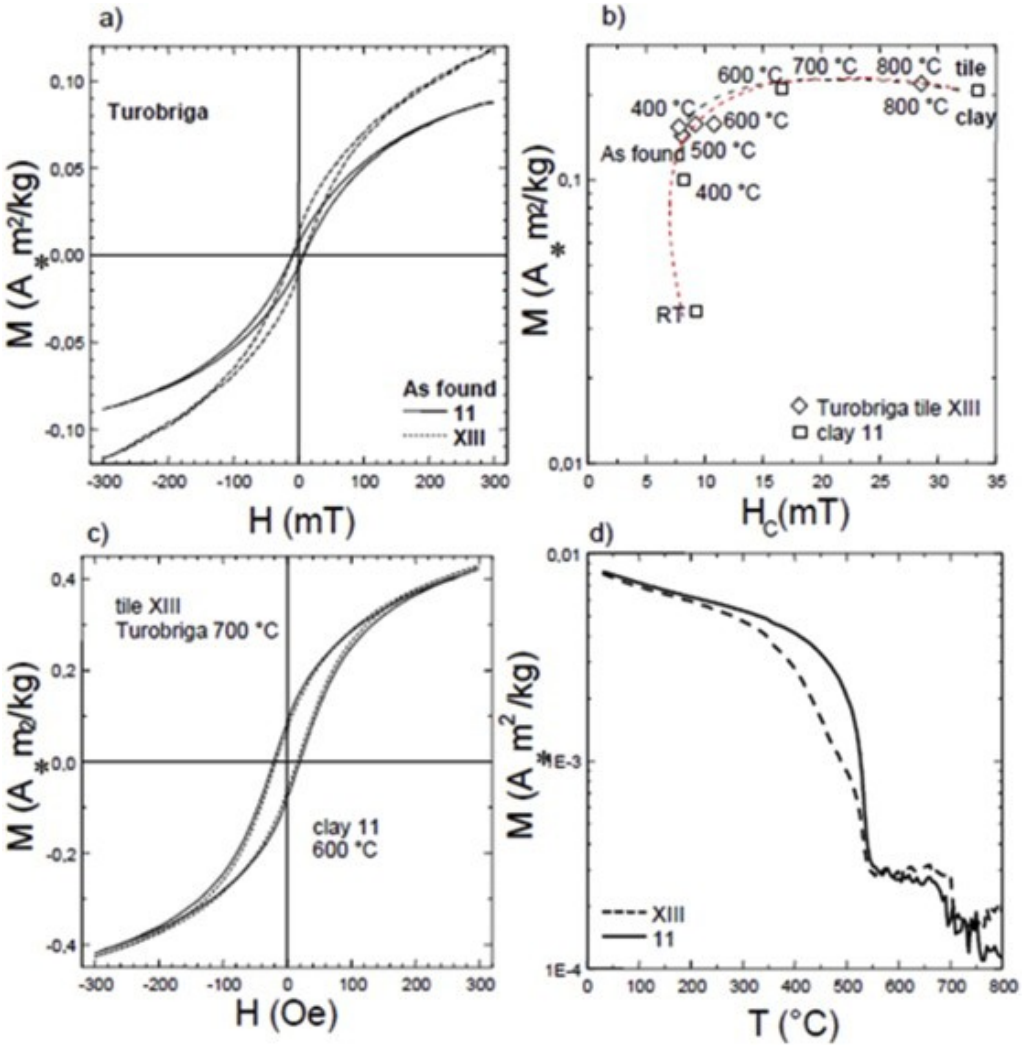

Fig. 9. a) Hysteresis loops at room temperature on as found samples from Andalusia (Spain): tile XIII and soil 11-Aroche. **b)** variation of the magnetic parameters, magnetization *vs*. coercive field, as a function of the applied thermal treatment temperature, **c)** hysteresis loops after thermal treatment at 700 °C and 600 °C respectively on clay 11 and tile XIII samples, **d)** thermomagnetic curve up to 800 °C on tile XIII and clay 11, treated up to 800 °C.

In Fig. 10, the same comparison as in Fig. 9 is made of the magnetic properties change versus temperature of soil 8 (corresponding to Cellarengo) and ceramic VI (*Hasta*), both located in the southeast area of the investigated region (Fig. 1). Fig. 10a shows the large difference in the magnetic loops of the as found soil and ceramic samples. Fig. 10b shows that soil 8 enhances its stable ferromagnetic character only after treatment at 600 °C, while the ceramic sample changes its magnetic character after treatment at 700 °C, indicating a value between 600 °C and 700 °C as the equivalent ancient heating temperature, also for sample VI. Fig. 10c confirms the similarity to sample VI achieved by the magnetic curve of soil 8 after heating at 600 °C; Fig. 10d compares the two similar thermomagnetic curves.

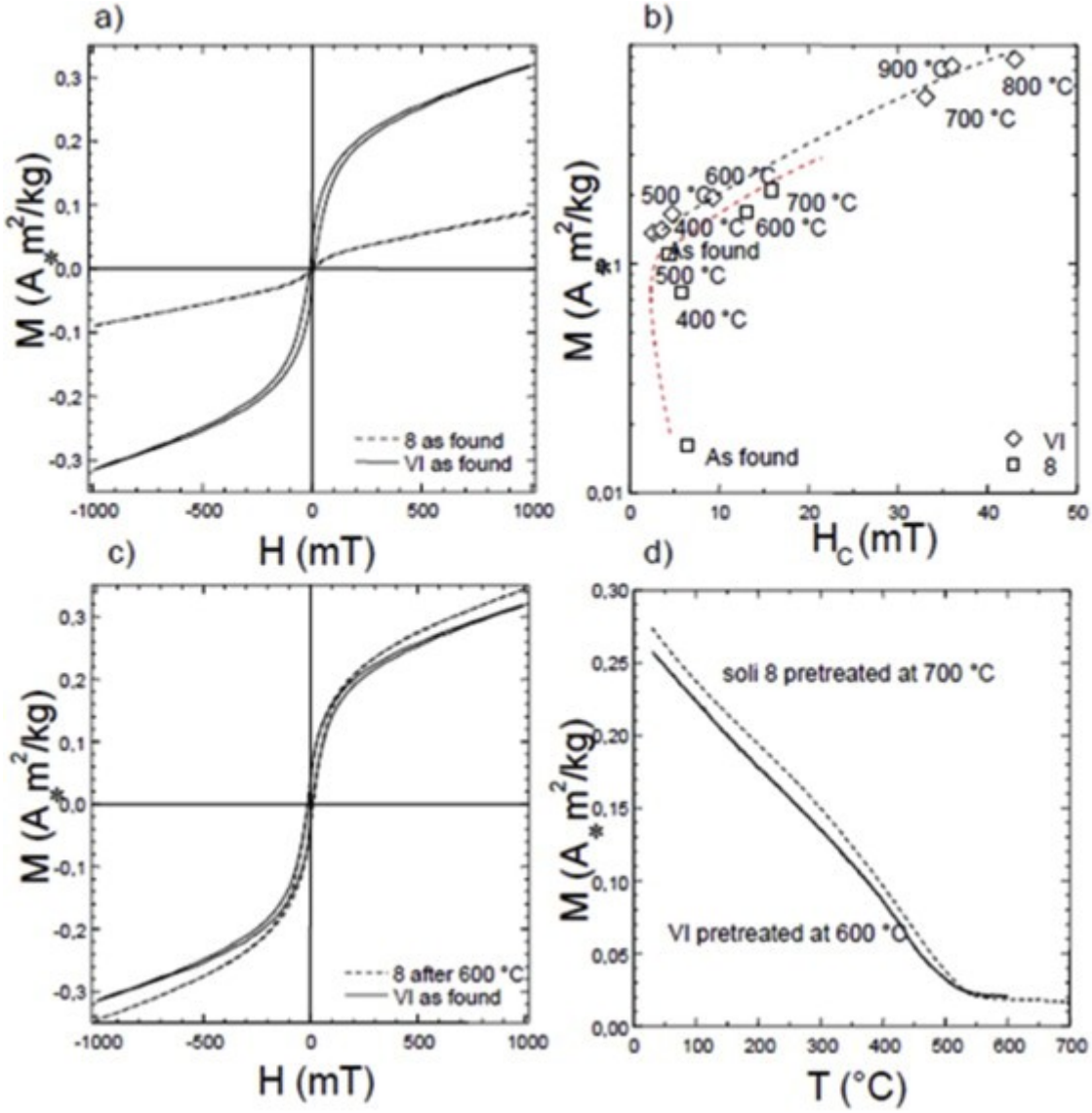

Fig. 10. a) Hysteresis loops at room temperature on as found samples from *Hasta* (brick VI) and Cellarengo (soil 8), **b)** variation of the magnetic parameters, magnetization *vs*. coercive field, as a function of the applied thermal treatment temperature, **c)** hysteresis loops for sample VI and soil 8 after thermal treatment at 600 °C, **d)** thermomagnetic curve for sample VI and soil 8, treated at 600 °C and 700 °C respectively.

The hysteresis curve of ceramic IV (Fig. 11), found at Brandizzo, suggests an important contribution to the magnetic moment of this sample due to small (paramagnetic and superparamagnetic) iron particles associated with more stable ferrimagnetic grains, probably made of Ti-magnetite. As magnetization increase is linear with the applied field below 300 mT, contributions due to hematite-like minerals are excluded. When compared with other ceramic samples, colour and magnetic properties of sample IV suggest that thermal treatment was carried out at temperatures not higher than 750–800 °C.

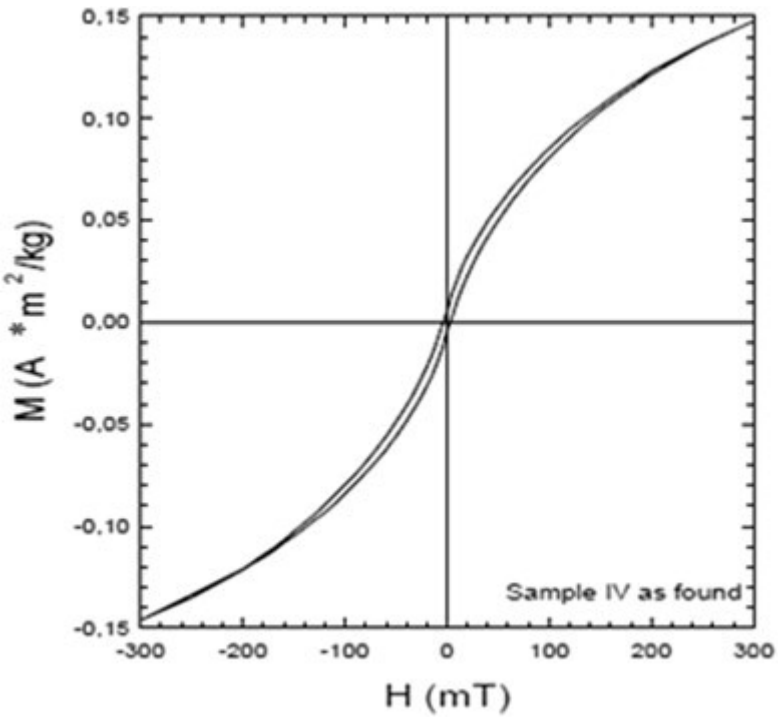

Fig. 11. Magnetization curve of the archaeological tile IV (Brandizzo), as found, with stamp M•A•[H].

3.4. Transformation of the soil mineralogy in the consequence of heating

Applying thermal treatments at different temperatures on the reference clays, directly in the thermal chamber of the XRD instrument or in a conventional furnace, we observed significant differences. Several differentiated parameters are able to explain this: *e.g.* in the XRD thermal chamber the amount of sample is small and the heating kinetics relatively fast, while the sample cannot fill completely the volume of the chamber, as in a conventional furnace. Probably due to these reasons, at any given temperature, the disappearance of primary minerals and the crystallization of secondary phases always attain upper grade in the conventional furnace (Fig. 7b). It is possible that the XRD chamber conditions only allow for a metastable state (data not shown). The mineralogy of crude soil 5-Vauda is composed of quartz and plagioclase (albite probably) as major components associated with minor phases as micas, amphibole (hornblende) and K-feldspar (Table 8). After 750 °C heating, the 14.1 Å reflection disappears because chlorite is unstable over 600 °C while a reflection appears close to 9.3 Å is interpreted possibly as talc or pyrophyllite crystallisation. On the other hand, the major peak of plagioclase decreases, which can indicate the beginning of the eutectic transition of this feldspar (Fig. 12). The mineralogical composition of soil 8 before thermal treatment is the same as soil 5, except for goethite. After heating, no 9.3 Å reflecting phase has crystallized and the reflection of the micas (9.7 Å) has disappeared. For soil 5 at 750 °C, the presence of hematite is doubtful because the major peak of this phase is in the same angular position as other phases. The mineralogy of soil 9 after thermal treatment confirms the composition of soil 8 but for a higher content in micaceous phases (10.0 Å). The broad tails of this peak probably indicate a contribution of dehydrated smectite phase.

Table 8. XRD soil 5-Vauda within the range of temperatures 680–1100 °C.

Temp/°C	t/h	Atm[a]	Color	Q[b]	FK	P	F	Hb	Sm	Ch	M1	M2	I	Ho	Go	He	Ca	Do	Ge	Py	Mu
60	12	ox	10YR 6/4	+++	++	++			(+)	++	+	+	(+)		(+)						
680	6	ox	2.5YR 5/8	+++	+	+			(+)	(+)	(+)	(+)	(+)			(+)					
750	12	ox	2.5YR 5/8	+++	+	+										+					
950	4	ox	2.5YR 5/8	+++	+	(+)										+					(+)
1070	2	ox	10R 4/6	++			(+)									+					+
1100	12	red	7.5YR 2/1	*												+					++

[a] Atm, atmosphere. ox, oxidising; red, reducing atmosphere obtained by OM rich unfired bricks according to Wolf (2002).

[b] Q (quartz), FK (K-feldspath), F (exsolution feldspars), P (plagioclase), Hb (amphibole), Sm (smectite), Ch (chlorite), M1 (muscovite-like), M2 (paragonite-like), I (illite), Ho (hornblende), Go (goethite), He (hematite), Ca (calcite), Do (dolomite), Ge (gehlenite), Py (pyroxene), Mu (mullite). (*) vitreous phase. In parenthesis poorly crystalline phases, bold high crystallinity.

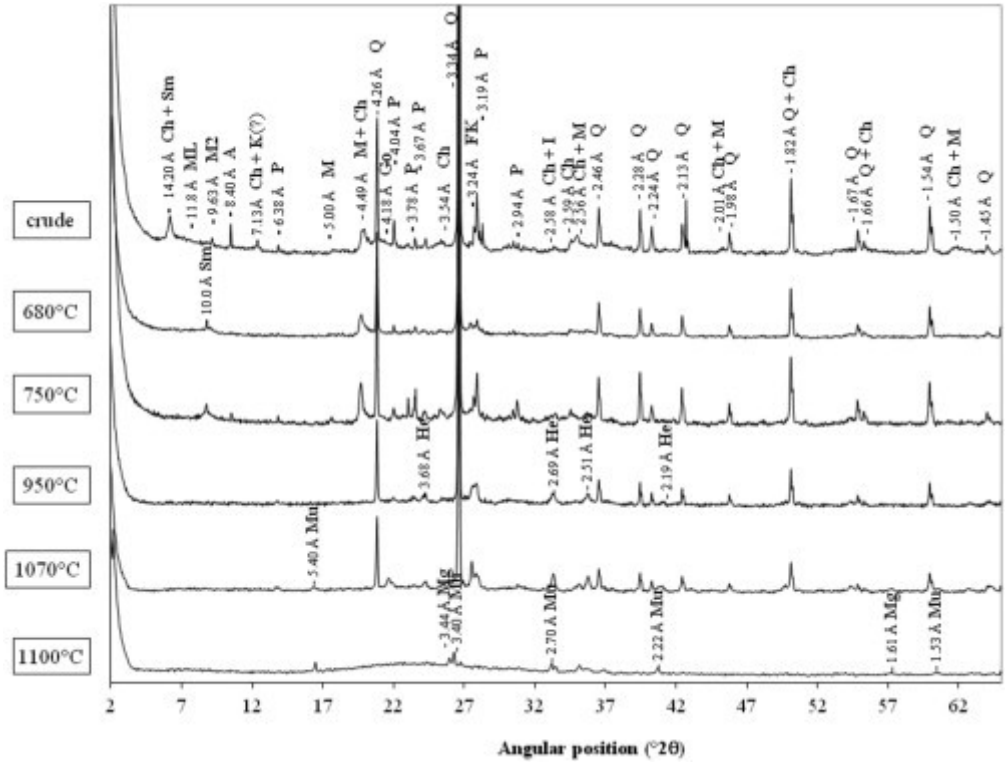

Fig. 12. Patterns of X-ray diffraction powders of soil 5-Vauda heated up to 1100 °C. The mineral phases successively identified are: smectite (Sm), chlorite (Ch), mixed-layer (ML), illite (I), muscovite-like (M1), paragonite-like (M2), kaolinite (K) quartz (Q), feldspar K (FK), plagioclase (P), goethite (Go), hematite (He), magnetite (Mg) and mullite (Mu).

The mineralogy of brick IV (Brandizzo) is essentially composed of quartz with low contents of feldspar minerals (K-feldspar and plagioclase), with broad peaks (3.24 Å and 3.19 Å respectively) possibly interpreted as a beginning of fusion (over the eutectic point temperature), and traces of amphibole (hornblende probably). Compared with crude clay before the 750 °C thermal treatment, the mineralogy of brick IV is without a phyllosilicate assemblage (chlorite, mica and probably smectite), differing from all 750 °C soil showing a reflection close to 10.0 Å, attributed to mica and dehydrated smectite. Another important difference is the high content in iron oxide (hematite) in brick IV, a mineral whose presence is always doubtful in experimentally heated soil samples (Fig. 12) as the kinetics of heating process is generally too fast to obtain a well crystallized phase.

The FTIR analysis provides additional information, complementary to XRD analysis. In the 1100–400 cm^{-1} region, bands corresponding to Si–O and Si–O–Si, and Al–O and Al–O–Al were detected in all of the archaeological samples. These vibrational bands could be attributed to the muscovite, feldspars, and quartz.

Appearance of bands at 1096 cm^{-1} and 630 cm^{-1} could be used as FTIR reflectance spectra indicators of previous heating treatment in the temperature range 400–550 °C (Berna et al., 2012). In contrast, the mid-IR spectra of the soil and of the soil samples heated up to 950 °C are similar. The mid-IR spectra of the soil 5 samples heated at 680 and 950 °C are very similar to the bricks II and VI spectra. The only difference comes from calcite (bands at about 1450, 875) whose occurrence is apparent in the bricks, but not in the heated samples. This is in accordance with the XRD data (Table 6, Table 7). The near-IR spectra of the soil heated at 680 °C is similar to bricks II and VI (Fig. 13). The NIR spectra of the soil 5 samples heated at 680 and 950 °C are very similar as well to the brick XI spectra. The only difference is the kaolinite disappearance for the heated samples; disappearance of the bands due to kaolinite at about 3700 and 3620 cm^{-1} (Fig. 14a). The spectrum of the sample heated at 1100 °C clearly differs. It reveals broad bands due to vitrification of the minerals (Fig. 14a and b). These analogies confirm the matching between Roman bricks and most probable soils utilised as raw material based on the REY_{UCC} pattern (Table 5).

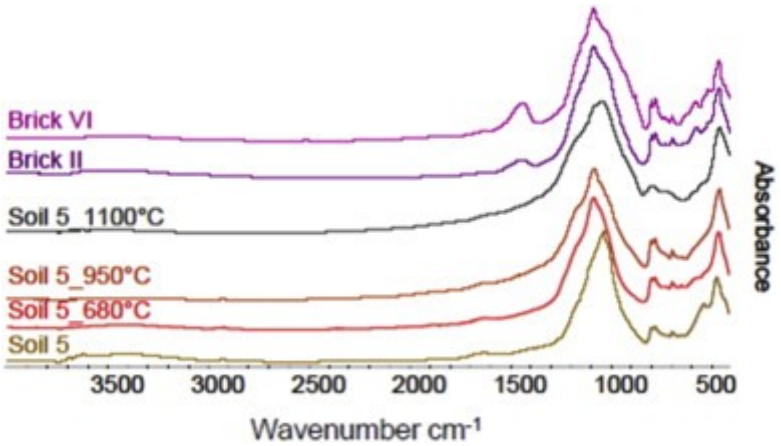

Fig. 13. FTIR spectra. Bricks II-*Segusio* and VI-*Hasta* compared to their most probable source, soil 5-Vauda fired within the temperature range 680–1100 °C.

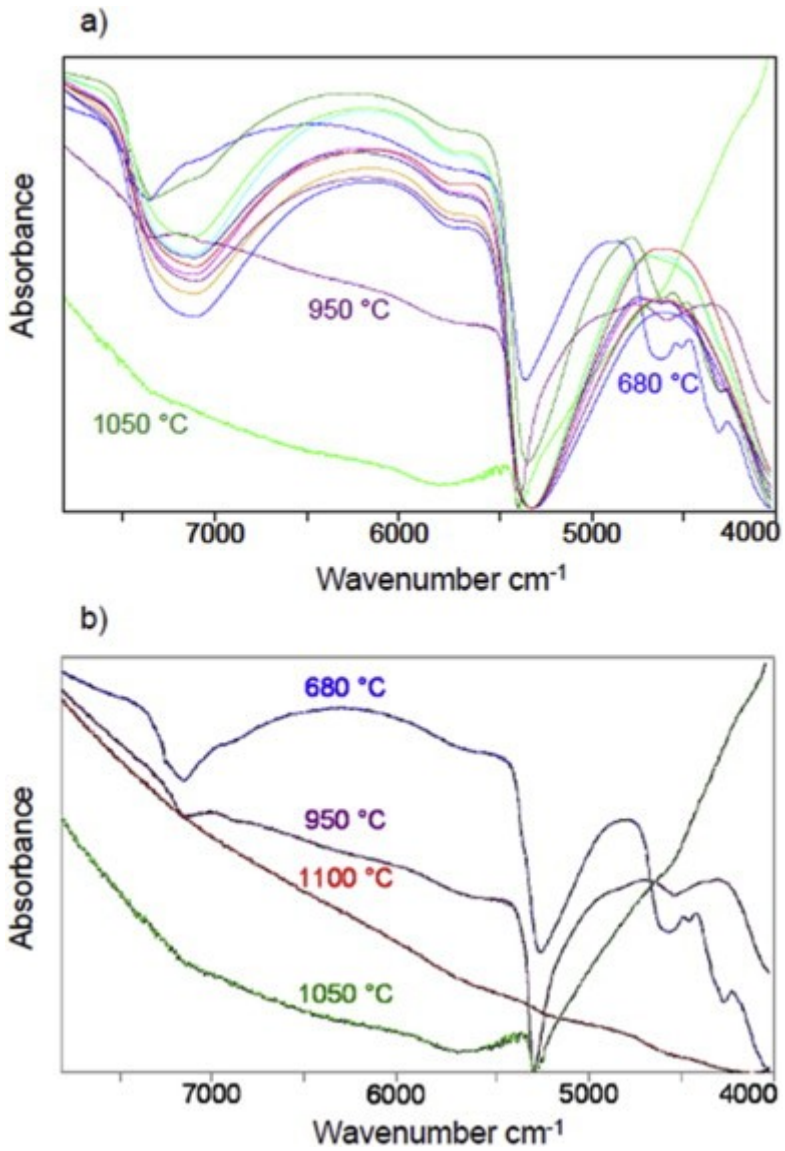

Fig. 14. NIR spectra. **a)** Archaeological samples of four tiles and four bricks from the same site of sample XI-*Industria* compared to soil 5-Vauda fired at different temperatures. **b)** Soil 5-Vauda fired within the temperature range 680–1100 °C.

4. Discussion

The samples examined show a close correlation between the point of use and discovery and soils from which they originated. Moreover, the lack of additives in the mixtures shows that the production of bricks was little influenced by the location of the resource “clay”, but much more by that of water and, above all, fuel for the furnaces. Woodland areas were not generally part of the lands granted to settlers as commons use by the community for cutting wood (*silva publica*) (Settis, 1984). The assumption, therefore, must be that bricks were produced in a short distance from places of employment and exceptional cases (other known brands in other areas, no structures in the locality where the predominant soil types is found, or prevailing use of stone in the buildings) must be analyzed on the basis of historical data available for the individual sites. In the Roman Empire, forest clearance occurred fundamentally for obtaining arable land but also retrieving wood for other uses and as a consequence, the Mediterranean underwent intensive deforestation (Wertime, 1983, Williams, 2000, Certini and Scalenghe, 2011). During Roman times in northern Italy, more than one third of the mountain forest cover disappeared and two thirds of the floodplain was cleared (Cremaschi et al., 1994, Drescher-Schneider, 1994, Cremonini et al., 2013). Nevertheless, the extent of deforestation (Farabegoli et al., 2004, Kaplan et al., 2009, Zanchetta et al., 2013), although not influenced primarily by the brick-making industry, was probably a consequence of it.

4.1. Brick-making technology

Sun-baked and unfired brick use dated from the beginning of the Holocene in the Middle East (Velde and Druc, 1999). The technology of firing bricks arrived probably centuries later from Mesopotamia to Europe and China, where sections of the Great Wall were partly built with burned bricks, and through the Middle East it reached Persia and India. In Europe, the Romans emulated their first expertise in building from the Etruscans (Ducati, 1927), although Greek influence was maintained in sizing. Being cheaper than stone-working, brick-making became during Roman times one of the most important industries and a state monopoly under the Empire (Coarelli, 2000). The Romans refined the Etruscan brick-making technology in the selection and preparation of the raw material and in the design of the kilns.

The soil material in modern brickmaking, once extracted, is left ventilating indoor for a few months (maturation). The purpose is to regulate the humidity of the material before firing, to avoid fractures. There is no analysis to confirm that the 'maturation' of the soil dug before cooking a modern brick also occurred in Roman times. Nor it is possible to determine analytically on a two thousand years old sesquipedalian brick that this practice was certainly adopted, but it is likely that a 'fermentation' or 'maturation' was already in use at the time of the Romans. After grinding, tempering, moulding, drying, and dressing, bricks were fired until the requisite hardness was obtained, conferring on them a resistance to weathering comparable to those of stones, which were much more difficult to work.

The terrigenous materials must be mixed with water to form the finished product, and the amount of added water depends on the nature and plasticity of the soils in addition to the temperature and air currents. The bricks, after being manufactured, must be dried as they could burst if heated without drying. Today, bricks are manufactured by mixing soils with water to attain plastic mechanical properties, then squeezing them with pressures as high as thousands kPa in rectangular steel columns, and finally cutting the individual units. Romans formed bricks using more water than today and placed the plastic mixture in wooden molds lubricated with sand or water. There is evidence that the raw soil material would have not required any addition but homogenisation only (Benea et al., 2010, Eramo and Maggetti, 2013).

Bricks are normally fired in a continuous oven-type chamber. The maximum temperature practically attainable is 1100 °C after one week of burning. Romans used heated enclosures as up-draught periodic kilns that, although being designed essentially on insulation, obtained a poor internal temperature distribution and hence an irregular firing of the bricks inside. The bottom part of the kiln adjacent to the firebox experienced higher internal temperature (T ~ 1100 °C). Heating was reduced gradually as naturally occurring convection fluxes conveyed heat towards the top of the kiln, approximately at a temperature lower than 800 °C, equivalent to the highest temperature of a small bonfire. Within the kiln, only 10% of bricks experienced temperatures higher than 950 °C or lower than 650 °C (Wolf, 2002). The principal determinant of the capacity of a brick factory is, and probably was, the size and number of kilns; in ancient times, it was also the availability of wood. Brick plants built during the 1960s had a production capacity of approximately 20 million extruded bricks per year, and a modern brick plant can produce 100 million bricks per year (Scheibl and Wood, 2005). Kiln functioning is today the bottleneck of brick production, and probably it was the same in ancient times.

The internal volume of Roman kilns probably ranged between 5 and 40 m^3 (Jackson et al., 1973, Darvill and McWhirr, 1984). The few Roman kilns for bricks discovered in Piedmont have cooking chambers approximately measuring 11–14 m^2, and their height is unknown. A chamber of 9 m^2 has a batch capacity of 3500 tiles (Barberan et al., 2002). The kilns burnt thousands of cubic meters of wood, at a rate as high as hundreds of cubic meters per year.

Estimating the manpower required in ancient time to form a brick is quite difficult. The labour force constraints in the brick-making industry pose different questions. The time required during Roman times for digging (including the unknown average depth), processing and firing have been only conjectured. For this reason, we shaped sesquipedalian bricks (45 × 30 × 10 cm) in wooden boxes in order to provide hypotheses

on the labour requirement for brick production. In our replica experiment (Fig. 3a) independent of the type of soil, full processing (excluding digging and firing) takes one unskilled man–day for ten *sesquipedales*, roughly 1000 *sesquipedales* for 1 skilled man–month applying an unskilled/skilled coefficient of 0.4 (Delaine, 2001).

4.2. Structural transformations during the firing of bricks

The soils of the study area contain quartz, plagioclase, chlorite, muscovite-like and paragonite-like minerals (Fig. 7b). Some of them contain K-feldspar, smectite, illite, hornblende, and goethite (Table 7). The only differences in comparison with Roman bricks are the lack of paragonite-like minerals and the sparse appearance of gehlenite and pyroxene (Table 6, Table 7). Most of the change in mineralogy occurs between 680 and 750 °C (Table 9, Fig. 10b). When the assemblage of aluminium silicates, iron oxides, organic carbon and carbonates, and other more soluble salts of a soil is fired at an appropriate temperature, irreversible chemical changes take place (Wolf, 2002). The final product turns, in general, into a durable material through transformations that develop with temperature (Table 9):

- heating to moderate temperatures below 300 °C enhances the magnetic fabric in bricks (Hus et al., 2002);
- maghemite may form at temperatures >300 °C (*e.g.* when “green” wood is used for firing, because of the reducing atmosphere created by the smoke emitted by this fuel; Gendler et al., 2005; Setti et al., 2006);
- below 400 °C, if the soil material is oxidized, porosity increases (if the heating takes place under reducing conditions, the remaining carbon turns into dark charcoal filling the pores);
- between 400 and 650 °C, dehydration takes place, OH-groups are removed from the structure of silicates and these hydroxyls are lost into the atmosphere, irreversibly altering clays and metal oxides (in ancient times, bricks were fired to temperatures commonly above 600 °C);
- above 700 °C clayey material is considered definitely fired. Well-fired pottery turns virtually inert and durable, assuming a reddish colour, confirmed by the presence of hematite;
- kaolinite may turn thermally into a ‘slightly disordered’ metakaolin just above 800 °C (Murad and Wagner, 1991) when all carbonates eventually present are lost and iron oxides turn entirely red and become a very stable material with a porosity higher than 20%. Increasing vitrification results in diminished porosity;
- spinel structures can form over 900 °C (bricks are then blackened or greyed if the atmosphere in the kiln is converted into reducing conditions, mainly due to organic matter conversion into unburned carbon particles);
- at temperatures higher than 900 °C the incipient vitrification reduces the porosity (which at 1100 °C is reduced to less than 5%); large earthenware vessels were fired at such high temperatures for purposes of sealing them;
- illite/muscovite disappear completely above 950 °C (Benea et al., 2010, Cultrone et al., 2011) while, depending on the initial composition of the raw material, mullite, gehlenite, and diopside begin to appear (when temperatures exceed 900 °C the presence of calcite enhances the stability of newly-formed gehlenite, which may persist up to 1075 °C, after that the degree of anisotropy of magnetic susceptibility decreases; Hus et al., 2002, Maniatis et al., 1981, Maniatis et al., 1983, Setti et al., 2006);
- at 1200–1300 °C, the highest temperature attainable in most ancient kilns, a very strong and translucent ceramic material occurs, stoneware, with a total porosity <2%;

- above these temperatures, total melting is expected (temperatures improbable to be attained in antiquity; Goffer, 2007; Pollard and Heron, 2008).

Table 9. Temperature De Boer and Dekkers, 2001, Dunlop and Ozdemir, 1997, Echajia et al., 2006, Khalfaoui and Hajjaji, 2009, Lopez-Arce and Garcia-Guinea, 2005, López et al., 2008, Morris, 1994, Rathossi and Pontikes, 2010, Rice, 1987, Rye, 1981, Schwertmann and Cornell, 2000, Velde and Druc, 1999, Zdujic et al., 1998 of decompositions and neoformations. Mineral neoformation (empty histograms, mineral in italics), beginning of instability (bars, minerals in bold), and some Curie temperatures (T_C). Scale in Celsius degrees.

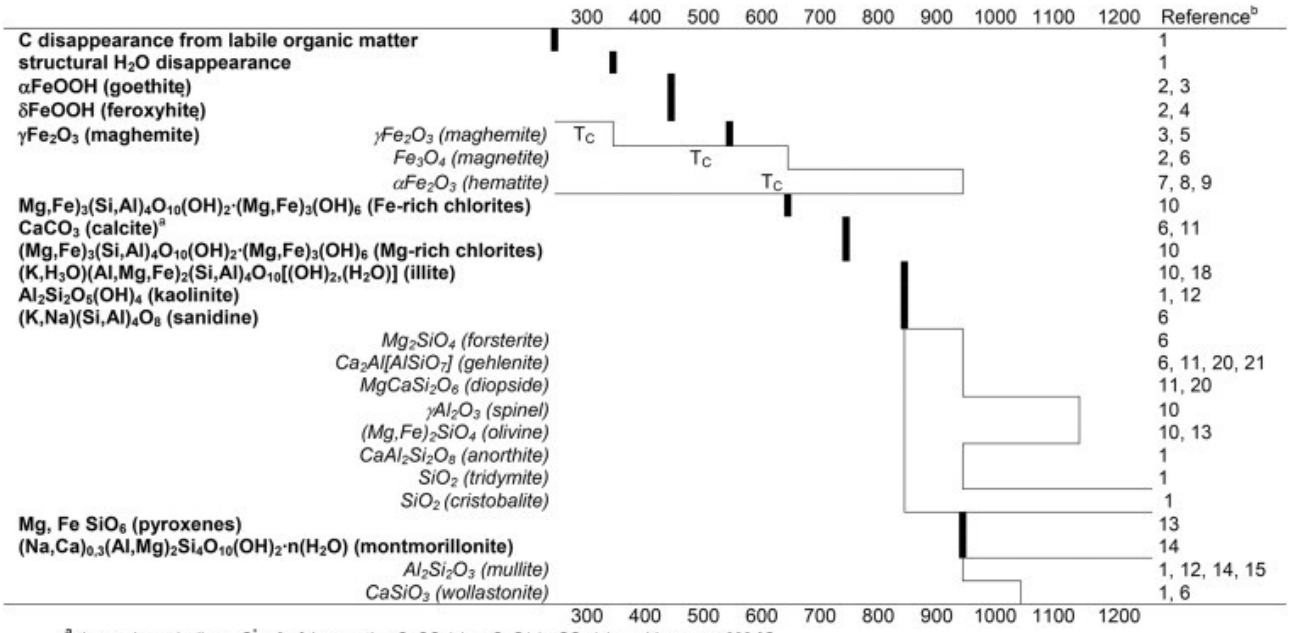

[a] thermodynamically a $\Delta G^{\circ} = 0$ of the reaction $CaCO_3(s) \rightarrow CaO(s) + CO_2(g)$ would occur at 833 °C

[b] references: 1) Velde and Druc (1999), 2) Schwertmann and Cornell (2000), 3) López et al. (2008), 4) Weckler and Lutz (1998), 5) Gendler et al. (2005), 6) Rathossi and Pontikes(2010), 7) De Boer and Dekkers (2001), 8) Morris (1994), 9) Zdujic et al. (1998), 10) Khalfaoui and Hajjaji (2009), 11) Lopez-Arce and Garcia-Guinea (2005), 12) Murad and Wagner (1991), 13) Echajia et al. (2006), 14) Rye (1981), 15) Rice (1987), 17) Dunlop and Ozdemir (1997), 18) Cultrone et al. (2011), 19) Benea et al. (2010), 20) Maniatis et al. (1983), 21) Setti et al., 2006)

5. Conclusions

A synopsis of the three main questions addressed by this manuscript (1, where did the Romans collect the raw materials?; 2, how did they make their bricks?; 3 how far have they transported the bricks with respect to the furnaces?) could be that in Roman brick-making soil characteristics were not essential, as they transported raw soil material usually for distances of only a few kilometres. Key points in order of importance were availability of timber and water and soils without stones.

The Romans, after having clear-cut an area, used some soil horizons suitable for their direct transformation into fired and unfired bricks. These soil horizons in the foothills of the Alps were also certainly horizons of impediment to the growth of plants (*e.g.* argillic, fragipan). Because the ‘brick’ quarries presumably could not be very deep, after their logging and the removal of some soil horizons, the Romans established agriculture that was not in antagonism but in synergy with the brick industry. Archaeologists have not yet reported finding quarries of Roman age devoted entirely to the brick industry. Probably, this results from the subsequent transformation of the landscape, as the forest-agriculture shift remains more evident than small topographic anthropogenic remodelling, traces of which have been lost over two millennia.

The sesquipedalian brick has been culturally inherited from the Greeks who had developed bricks of this volume to build large, sometimes huge items. As no calculations were made in the structural design of buildings, their over-sizing was necessary and was easily obtained with sesquipedalian bricks. In addition to aesthetic and cultural reasons, there are geometric reasons and standardization constraints imposing the uncomfortable (from a technological point of view) size of a Roman brick. The type of soil did not affect the production technology of Roman bricks, which differs (very slightly) geographically only for cultural reasons.

Our idea explained in this work was to evaluate the predominately analytical techniques to verify the specific utility and their effectiveness in the specific case of bricks and tiles, summarising our findings compared to the current literature (Table 10). Bricks are ubiquitous materials and 'trivial' from an archaeological point of view. Rare are stamped bricks or tiles. For this reason, the only keys of archaeological investigation are not sufficient to clarify the suppositions about the originating materials used in the brick-making industry. This happens even when laboratory routine methods are coupled. *Per se*, the mineralogy of bricks, their content of major chemical elements, or their magnetic behaviour provides no information explaining the origin of raw material used.

Table 10. Brickmaking. Effectiveness of analytical techniques compared by groupings: archeological methods (ARCHEO), routine methods (ROUTINE), mineralogy and spectroscopy (MIN), magnetic (MAG), metals (MET), and Rare Earth Elements and yttrium (REY).

Type of technique[a]		**Origin of raw material**[b]	**Clues on technology**[b]
ARCHEO[c]	Epigraphy	■	●
	Prosopography	■	●
	Experimental archeology	■	●
	Shape	■	●
	Size	■	●
	Colour	■	●
	Stamps	■■■	●
ROUTINE	Soil in field	□	●●
	Chemical analyses	■	●
	Physical analyses	■■	●●
	OM	■	●●
	LOI	■	●
MIN	XRD	■	●●
	FTIR	■	●●
	DRIFT	■■	●●
	SEM-EDS	■	●●
	XRF	■■	●
	Raman spectroscopy	■	●●
MAG	Magnetization curves	■	●●●
	Saturation magnetization	■	●●
	Remanence	■	●●
MET	AAS	■■	○
	ICP-MS	■■	○
	EDAX	■■	○
	TOF-SIMS	■	●
REY	ICP-MS	■■■■	○○

a Optical microscopy **OM**, loss on ignition **LOI**, X-ray diffraction **XRD**, Fourier transform infrared spectroscopy **FTIR**, diffuse reflectance infrared Fourier transform spectroscopy **DRIFT**, scanning electron microscopy with energy dispersive spectrometer **SEM-EDS**, X-ray fluorescence **XRF**, atomic absorption spectroscopy **AAS**, inductively coupled plasma mass spectrometry **ICP-MS**, time-of-flight secondary ion mass spectrometry **TOF-SIMS**, energy dispersive spectrometer **EDAX**.

b ■/● fair, ■■/●● moderate, ■■■/●●● effective, ■■■■/●●●● very effective [open symbols means without evidence in the current Literature].

c The bricks are extremely standardized, ubiquitous materials and very 'trivial' from an archaeological point of view. Very rare are the stamped bricks or tiles.

In particular, only rare earth elements plus yttrium (REY) provide keys useful to help us understand the geographical origin of the materials used in the manufacture of bricks or tiles, even in the absence of archaeological evidence (*e.g.* furnaces). ICP-MS appears to be an ideal method to study archaeological samples because of its good detection limits, precisions, accuracies, and multi-elemental determination. Clues of the technology in the brick-making can only be reached by the combined use of different techniques: either more traditional ones, such as optical microscopy and diffraction, or more recent ones. In particular, magnetic techniques allow establishing with precision the maximum temperature to which the material has been subjected. Therefore, the possibility to discriminate the provenance regions opens new perspectives in the studies of archaeological bricks, and to understand the trade routes at different periods.

Acknowledgments

Region Poitou-Charentes (n°09/RPC-R055) kindly supported the first author. DISAFA-Università di Torino made its laboratories available for some of the analyses. ARPA Piemonte has provided data on the Gd/La ratio. Hamish Forbes and Giuseppina Spagnolo Garzoli provided extremely useful and valuable information. The Carena family from Cambiano kindly has made available its historical experience in the manufacture of bricks. Carlos Odriozola and Antonio Delgado from the Universidad de Sevilla provided the Andalusian samples. We are further indebted to Rosanna Nardi for providing Fig. 2b. We wish to express extreme gratitude to Peter Randerson from Cardiff University for the time he generously devoted to reading and reviewing this manuscript.

Appendix A. Supplementary data

Supplementary data on major chemical elements (SI1) and on size of Roman bricks (SI2) related to this article can be found at http://dx.doi.org/10.1016/j.quaint.2014.11.026.

References

Alonso et al., 2012
E. Alonso, A.M. Sherman, T.J. Wallington, M.P. Everson, F.R. Field, R. Roth, R.E. Kirchain
Evaluating rare earth element availability: a case with revolutionary demand from clean technologies
Environmental Science & Technology, 46 (2012), pp. 3406-3414

Arnold, 1985
D.E. Arnold
Ceramic Theory and Cultural Process
Cambridge University Press, Cambridge (1985)

Atkinson and King, 2005
D. Atkinson, J.A. King
Fine particle magnetic mineralogy of archaeological ceramics
Journal of Physics: Conference Series, 17 (2005), pp. 145-149

Barberan et al., 2002
S. Barberan, O. Maufras, H. Petitot, H. Pomarèdes, L. Sauvage, R. Thernot
Les *villae* de La Ramière à Roquemaure, Gard
Monographies d'Archéologie Méditerranéen, 10 (2002), pp. 889-919
(in French)

Barello, 2004
F. Barello
Brandizzo – Un Insediamento Rurale di Età Romana
Edizioni Relazioni Esterne TAV, Roma (2004)
(in Italian)

Beatrice et al., 2008
C. Beatrice, M. Coïsson, E. Ferrara, E.S. Olivetti
Relevance of magnetic properties for the characterisation of burnt clays and archaeological tiles
Physics and Chemistry of the Earth, 33 (2008), pp. 458-464

Benea et al., 2010
M. Benea, M. Gorea, N. Har
Tegular materials from Sarmizegetusa – 2. Mineralogical and physical characteristics of the raw material
Romanian Journal of Materials, 40 (2010), pp. 228-236

Berna et al., 2012
F. Berna, P. Goldberg, L.K. Horwitz, J. Brink, S. Holt, M. Bamford, M. Chazan

Microstratigraphic evidence of in situ fire in the Acheulean strata of Wonderwerk Cave, Northern Cape province, South Africa
Proceedings of the National Academy of Sciences, 109 (2012), pp. E1215-E1220

Biasioli et al., 2012
M. Biasioli, G. Fabietti, R. Barberis, F. Ajmone-Marsan
An appraisal of soil diffuse contamination in an industrial district in northern Italy
Chemosphere, 88 (2012), pp. 1241-1249

Bouchez et al., 1974
R. Bouchez, J. Coey, R. Coussement, K. Schmidt, M. Van Rossum, J. Aprahamian, J. Deshayes
Mössbauer study of firing conditions used in the manufacture of the grey and red ware of Tureng-Tepe
Journal of Physique, 35 (1974), pp. 541-546

Braun et al., 1993
J.J. Braun, M. Pagel, A. Herbillon, C. Rosin
Mobilization and redistribution of REEs and thorium in a syenitic lateritic profile – a mass-balance study
Geochimica et Cosmochimica Acta, 57 (1993), pp. 4419-4434

Caitcheon, 1993
G.G. Caitcheon
Applying environmental magnetism to sediment tracing
N. Peters, E. Hoehn, C. Leibundgut, N. Tase, D. Walling (Eds.), Tracers in Hydrology, International Association of Hydrological Sciences, Wallingford (1993), pp. 285-292

Calliari et al., 2001
I. Calliari, E. Canal, L. Cavazzoni, S. Lazzarini
Roman bricks from the Lagoon of Venice: a chemical characterization with methods of multivariate analysis
Journal of Cultural Heritage, 2 (2001), pp. 23-29

Certini and Scalenghe, 2011
G. Certini, R. Scalenghe
Anthropogenic soils are the golden spikes for the Anthropocene
The Holocene, 21 (2011), pp. 1269-1274

Coarelli, 2000
F. Coarelli
L'inizio dell'*opus testaceum* a Roma e nell'Italia romana
P. Boucheron, H. Broise, Y. Thébert (Eds.), La Brique Antique et Médiévale. Production et Commercialisation d'un Materiau, École Française, Roma (2000), pp. 87-95
(in Italian)

Coey et al., 1979
J. Coey, R. Bouchez, N.V. Dang
Ancient techniques
Journal of Applied Physics, 50 (1979), pp. 7772-7777

Cremaschi et al., 1994
M. Cremaschi, M. Marchetti, C. Ravazzi
Geomorphological evidence for land cleared from forest in the central Po plain (Northern Italy) during the Roman period
B. Frenzel (Ed.), Evaluation of Land Surfaces Cleared from Forest in the Mediterranean Region during the Time of the Roman Empire, Gustav Fischer Verlag, Stuggart (1994), pp. 119-132

Cremonini et al., 2013
S. Cremonini, D. Labate, R. Curina
The late-antiquity environmental crisis in Emilia region (Po river plain, Northern Italy): geoarchaeological evidence and paleoclimatic considerations
Quaternary International, 316 (2013), pp. 162-178

Cultrone et al., 2011
G. Cultrone, E. Molina, C. Grifa, E. Sebastián
Iberian ceramic production from Basti (Baza, Spain): first geochemical, mineralogical and textural characterization
Archaeometry, 53 (2011), pp. 340-363

Dalan and Banerjee, 1998
R.A. Dalan, S.K. Banerjee
Solving archaeological problems using techniques of soil magnetism
Geoarchaeology, 13 (1998), pp. 3-36

Darvill and McWhirr, 1984
T. Darvill, A. McWhirr
Brick and tile production in Roman Britain: models of economic organisation
World Archaeology, 15 (1984), pp. 239-261

De Boer and Dekkers, 2001
C.B. De Boer, M.J. Dekkers
Unusual thermomagnetic behaviour of haematites: neoformation of a highly magnetic spinel phase on heating in air
Geophysical Journal International, 144 (2001), pp. 481-494

Delaine, 2001
J. Delaine
Exploring the economics of building techniques at Rome and Ostia
D.J. Mattingly, J. Salmon (Eds.), Economies beyond Agriculture in the Classical World, Routledge, Abingdon (2001), pp. 230-268

Drescher-Schneider, 1994
R. Drescher-Schneider
Forest, forest clearance and open land during the time of the Roman empire, in northern Italy (the botanical record)
B. Frenzel (Ed.), Evaluation of Land Surfaces Cleared from Forest in the Mediterranean Region during the Time of the Roman Empire, Gustav Fischer Verlag, Stuggart (1994), pp. 23-58
Ducati, 1927
P. Ducati
Storia dell'Arte Etrusca
Rinascimento del Libro, Firenze (1927)
(in Italian)
Dunlop and Ozdemir, 1997
D.J. Dunlop, O. Ozdemir
Rock Magnetism. Fundamentals and Frontiers
Cambridge University Press, Cambridge (1997)
Ebihara and Miura, 1996
M. Ebihara, T. Miura
Chemical characteristics of the Cretaceous-Tertiary boundary layer at Gubbio, Italy
Geochimica et Cosmochimica Acta, 60 (1996), pp. 5133-5144
Echajia et al., 2006
M. Echajia, S. Kacim, M. Hajjaji
Structural change and firing characteristics of a dolomitic clay
Annales de Chimie-Science des Materiaux, 31 (2006), pp. 23-30
Eramo and Maggetti, 2013
G. Eramo, M. Maggetti
Pottery kiln and drying oven from *Aventicum* (2nd century AD, Ct. Vaud, Switzerland): raw materials and temperature distribution
Applied Clay Science, 82 (2013), pp. 16-23
Facchinelli et al., 2001
A. Facchinelli, E. Sacchi, L. Mallen
Multivariate statistical and GIS-based approach to identify heavy metal sources in soils
Environmental Pollution, 114 (2001), pp. 313-324
Farabegoli et al., 2004
E. Farabegoli, G. Onorevoli, C. Bacchiocchi
Numerical simulation of Holocene depositional wedge in the southern Po Plain-northern Adriatic Sea (Italy)
Quaternary International, 120 (2004), pp. 119-132
Fouzai et al., 2012
B. Fouzai, L. Casas, N.L. Ouazaa, A. Álvarez
Archaeomagnetic data from four Roman sites in Tunisia
Journal of Archaeological Science, 39 (2012), pp. 1871-1882
Gendler et al., 2005
T.S. Gendler, V.P. Shcherbakov, M.J. Dekkers, A.K. Gapeev, S.K. Gribov, E. McClelland
The lepidocrocite-maghemite-haematite reaction chain–I. Acquisition of chemical remanent magnetization by maghemite, its magnetic properties and thermal stability
Geophysical Journal International, 160 (2005), pp. 815-832
Gliozzo, 2013
E. Gliozzo
Stamped bricks from the *ager cosanus* (Orbetello, Grosseto): integrating archaeometry, archaeology, epigraphy and prosopography
Journal of Archaeological Science, 40 (2013), pp. 1042-1058
Goffer, 2007
Z. Goffer
Archaeological Chemistry
(Second edn.), Wiley, Hoboken (2007)
Hatcher et al., 1994
H. Hatcher, A. Kaczmarczyk, A. Scherer, R.P. Symonds
Chemical classification and provenance of some Roman glazed ceramics
American Journal of Archaeology, 98 (1994), pp. 431-456
Helen, 1975
T. Helen
Organization of Roman Brick Production in the First and Second Centuries AD: an Interpretation of Roman Brick Stamps
Suomalainen Tiedeakatemia, Helsinki (1975)
Henderson, 1984
P. Henderson
Rare Earth Element Geochemistry
Elsevier, Amsterdam (1984), pp. 1-29
Hodder, 2012
I. Hodder
Entangled
Wiley-Blackwell, Chicester (2012)

Hus et al., 2002
J. Hus, S. Ech-Chakrouni, D. Jordanova
Origin of magnetic fabric in bricks: its implications in archaeomagnetism
Physics and Chemistry of the Earth, 27 (2002), pp. 1319-1331
Jackson et al., 1973
D.A. Jackson, L. Biek, B.F. Dix
A Roman lime kiln at Weekley, Northants
Britannia, 4 (1973), pp. 28-140
Kaplan et al., 2009
J.O. Kaplan, K.M. Krumhardt, N. Zimmermann
The prehistoric and preindustrial deforestation of Europe
Quaternary Science Reviews, 28 (2009), pp. 3016-3034
Khalfaoui and Hajjaji, 2009
A. Khalfaoui, M. Hajjaji
A chloritic-illitic clay from Morocco: temperature-time-transformation and neoformation
Applied Clay Science, 45 (2009), pp. 3-89
La Borgne, 1965
E. La Borgne
Les proprietes magnetiques du sol. Application a la prospection des sites archaeologiques
Archaeo-Phyika, 1 (1965), pp. 1-20
(in French)
López et al., 2008
F.A. López, M.C. Ramirez, J.A. Pons, A. López-Delgado, F.J. Alguacil
Kinetic study of the thermal decomposition of low-grade nickeliferous laterite ores
Journal of Thermal Analysis and Calorimetry, 94 (2008), pp. 517-522
Lopez-Arce and Garcia-Guinea, 2005
P. Lopez-Arce, J. Garcia-Guinea
Weathering traces in ancient bricks from historic buildings
Building and Environment, 40 (2005), pp. 929-941
López-Arce et al., 2003
P. López-Arce, J. García Guine, M. Gracia, J. Obis
Bricks in historical buildings of Toledo City: characterisation and restoration
Materials Characterization, 50 (2003), pp. 59-68
Maggetti and Schwab, 1982
M. Maggetti, H. Schwab
Iron age fine pottery from Chatillon-s-Glane and the Heuneburg
Archaeometry, 24 (1982), pp. 21-36
Maniatis et al., 1981
Y. Maniatis, A. Simopoulos, A. Kostikas
Mössbauer study of the effect of calcium content on iron oxide transformations in fired clays
Journal of the American Ceramic Society, 64 (1981), pp. 263-269
Maniatis et al., 1983
Y. Maniatis, A. Simopoulos, A. Kostikas, V. Perdikatsis
Effect of reducing atmosphere on minerals and iron oxides developed in fired clays: the role of Ca
Journal of the American Ceramic Society, 66 (1983), pp. 773-781
Marengo et al., 2005
E. Marengo, M. Aceto, E. Robotti, M.C. Liparota, M. Bobba, G. Pantò
Archaeometric characterisation of ancient pottery belonging to the archaeological site of Novalesa Abbey (Piedmont, Italy) by ICP–MS and spectroscopic techniques coupled to multivariate statistical tools
Analytica Chimica Acta, 537 (2005), pp. 359-375
Marra et al., 2011
F. Marra, D. Deocampo, D. Jackson, G. Ventura
The Alban Hills and Monti Sabatini volcanic products used in ancient Roman masonry (Italy): an integrated stratigraphic, archaeological, environmental and geochemical approach
Earth-Science Reviews, 108 (2011), pp. 115-136
Meloni et al., 2000
S. Meloni, M. Oddone, N. Genova, A. Cairo
The production of ceramic material in Roman Pavia: an archeometric NAA investigation of clay sources and archaelogical artifacts
Journal of Radioanalytical and Nuclear Chemistry, 244 (2000), pp. 553-558
Mirti et al., 1990
P. Mirti, V. Zelano, R. Aruga, E. Ferrara, L. Appolonia
Roman pottery from *Augusta Praetoria*: a provenance study
Archaeometry, 32 (1990), pp. 163-175
Morris, 1994
A.H. Morris
Canted Antiferromagnetism: Hematite
World Scientific Publishing Company, London (1994)
Murad and Wagner, 1991
E. Murad, U. Wagner

Mössbauer spectra of kaolinite, halloysite and the firing products of kaolinite: new results and a reappraisal of published work
Neues Jahrbuch für Mineralogie, 162 (1991), pp. 281-309

Nardi, 2011
R. Nardi
I laterizi bollati da Industria
E. Zanda (Ed.), Industria. Città Romana Sacra a Iside, Umberto Allemandi & C, Torino (2011), pp. 143-145
(in Italian)

Nesbitt, 1979
H.W. Nesbitt
Mobility and fractionation of rare earth elements during weathering of a granodiorite
Nature, 279 (1979), pp. 206-210

Pollard and Heron, 2008
A.M. Pollard, C. Heron
Archaeological Chemistry
(second ed.), The Royal Society of Chemistry, Cambridge (2008)

Rathossi and Pontikes, 2010
C. Rathossi, Y. Pontikes
Effect of firing temperature and atmosphere on ceramics made of NW Peloponnese clay sediments. Part I: reaction path, crystalline phases, microstructure and colour
Journal of the European Ceramic Society, 30 (2010), pp. 1841-1851

Regione Piemonte, 2010
Regione Piemonte
Carta dei Suoli del Piemonte 1:250.000
(2010)
(in Italian). WebGIS at URL
www.regione.piemonte.it/agri/suoli_terreni/suoli1_250/carta_suoli/gedeone.do

Rice, 1987
P.M. Rice
Pottery Analysis: a Source Book
University of Chicago Press, Chicago (1987)

Rye, 1981
O.S. Rye
Pottery Technology: Principles and Reconstruction
Taraxacum, Washington DC (1981)

Saiano and Scalenghe, 2009
F. Saiano, R. Scalenghe
An anthropic soil transformation fingerprinted by REY patterns
Journal of Archaeological Science, 36 (2009), pp. 2502-2506

Scheibl and Wood, 2005
F. Scheibl, A. Wood
Investment sequencing in the brick industry: an application of grounded theory
Cambridge Journal of Economy, 29 (2005), pp. 223-247

Schiffer and Skibo, 1997
M.B. Schiffer, J.M. Skibo
The explanation of artifact variability
American Antiquity, 62 (1997), pp. 27-50

Schwertmann and Cornell, 2000
U. Schwertmann, R.M. Cornell
Iron Oxides in the Laboratory: Preparation and Characterization
Wiley-VCH, Weinheim (2000)

Setti et al., 2006
M. Setti, C. Nicola, A. López-Galindo, S. Lodola, C. Maccabruni, F. Veniale
Archaeometric study of bricks from the ancient defence walls around the town of Pavia in northern Italy
Materiales de Construcción, 56 (2006), pp. 5-23

Settis, 1984
S. Settis
Misurare la Terra: Centuriazione e Coloni nel Mondo Romano
Edizioni Panini, Modena (1984)
(in Italian)

Skibo and Feinman, 1999
J.M. Skibo, G.M. Feinman
Pottery & People. Foundations of Archaeological Inquiry
University of Utah Press, Chicago (1999)

Soil Survey Staff, 1999
Soil Survey Staff
Soil Taxonomy: a Basic System of Soil Classification for Making and Interpreting Soil Surveys
Handbook 436
(second ed.), Natural Resources Conservation Service of the United States Department of Agriculture, Washington DC (1999)

Tema, 2009

E. Tema
Estimate of the magnetic anisotropy effect on the archaeomagnetic inclination of ancient bricks
Physics of the Earth and Planetary Interiors, 176 (2009), pp. 213-223

Thébert, 2000
Y. Thébert
Transport à grande distance et magasinage de briques dans l'Empire Romain
P. Boucheron, H. Broise, Y. Thébert (Eds.), La Brique Antique et Médiévale. Production et Commercialisation d'un Matériau, École Française, Roma (2000), pp. 342-356

Van Klinken, 2001
J. Van Klinken
Magnetization of ancient ceramics
Archaeometry, 43 (2001), pp. 49-57

Velde and Druc, 1999
B. Velde, I.C. Druc
Archaeological Ceramic Materials: Origin and Utilization
Springer, Berlin (1999)

Weckler and Lutz, 1998
B. Weckler, H.D. Lutz
Lattice vibration spectra. Part XCV. Infrared spectroscopic studies on the iron oxide hydroxides goethite (α), akaganéite (β), lepidocrocite (γ), and feroxyhite (δ)
European Journal of Solid State and Inorganic Chemistry, 35 (1998), pp. 531-544

Wedepohl, 1995
H. Wedepohl
The composition of the continental crust
Geochimica et Cosmochimica Acta, 59 (1995), pp. 1217-1239

Wertime, 1983
T.A. Wertime
The Furnace versus the Goat: the pyrotechnologic industries and Mediterranean deforestation
Journal of Field Archaeology, 10 (1983), pp. 445-452

Williams, 2000
M. Williams
Dark ages and dark areas: global deforestation in the deep past
Journal of Historical Geography, 26 (2000), pp. 28-46

Wolf, 2002
S. Wolf
Estimation of the production parameters of very large medieval bricks from St. Urban, Switzerland
Archaeometry, 44 (2002), pp. 37-65

Yang et al., 1993
S. Yang, J. Shaw, T. Rolph
Archaeointensity studies of Peruvian pottery from 1200 BC to 1800 AD
Journal of Geomagnetism and Geoelectricity, 45 (1993), pp. 1193-1207

Zanda, 2007
E. Zanda
Tra Industria e Vardacate. L'Insediamento di Mombello e le Presenze di Età Romana in Valcerrina
Museo Civico, Casale Monferrato (2007)
(in Italian)

Zanchetta et al., 2013
G. Zanchetta, M. Bini, M. Cremaschi, M. Magny, L. Sadori
The transition from natural to anthropogenic-dominated environmental change in Italy and the surrounding regions since the Neolithic: an introduction
Quaternary International, 303 (2013), pp. 1-9

Zanda, 2011
E. Zanda
Industria – Città Romana Sacra a Iside
Umberto Allemandi & C, Torino (2011)
(in Italian)

Zdujic et al., 1998
M. Zdujic, C. Jovalekic, L. Karanovic, M. Mitric, D. Poleti, D. Skala
Mechanochemical treatment of α-Fe_2O_3 powder in air atmosphere
Materials Science Engineering, A245 (1998), pp. 109-117